EUROPEAN RESPIRATORY *journal*

FLAGSHIP SCIENTIFIC JOURNAL OF ERS

Early View

Original research article

The rescue of F508del-CFTR by elexacaftor/tezacaftor/ivacaftor (Trikafta) in human airway epithelial cells is underestimated due to the presence of ivacaftor

Frédéric Becq, Sandra Mirval, Thomas Carrez, Manuella Lévêque, Arnaud Billet, Christelle Coraux, Edouard Sage, Anne Cantereau

Please cite this article as: Becq Fédéric, Mirval S, Carrez T, *et al*. The rescue of F508del-CFTR by elexacaftor/tezacaftor/ivacaftor (Trikafta) in human airway epithelial cells is underestimated due to the presence of ivacaftor. *Eur Respir J* 2021; in press (https://doi.org/10.1183/13993003.00671-2021).

The rescue of F508del-CFTR by elexacaftor/tezacaftor/ivacaftor (Trikafta) in human airway epithelial cells is underestimated due to the presence of ivacaftor.

Frédéric Becq[1], Sandra Mirval[1], Thomas Carrez[1,2], Manuella Lévêque[1], Arnaud Billet[1], Christelle Coraux[3], Edouard Sage[4,5], Anne Cantereau[1]

[1] Laboratoire Signalisation et Transports Ioniques Membranaires, Université de Poitiers, F-86073, France.

[2] ManRos therapeutics, Presqu'île de Perharidy, 29680 Roscoff, France.

[3]INSERM UMR-S 1250, Université de Reims-Champagne Ardenne, Reims, 51100, France.

[4]INRAE UMR 0892, Université Versailles-Saint-Quentin-en-Yvelines, Versailles, 78000, France.

[5]Service de chirurgie thoracique et transplantation pulmonaire, Hôpital Foch, Suresnes, 92150, France.

Corresponding author: Frédéric Becq, PhD, Laboratoire STIM, Université de Poitiers, Bâtiment B36, Pôle Biologie Santé, 1 rue Georges Bonnet, TSA 51106, 86073 Poitiers, France.

Tel: (33) 549 45 37 29 ; Email : frederic.becq@univ-poitiers.fr

Keywords: Cystic Fibrosis, Trikafta, VX445, VX661, VX809, VX770, F508del-CFTR

Tweetable abstract @ERSpublications

Trikafta, the modulator therapy for Cystic Fibrosis (CF) is elexacaftor+tezacaftor+ivacaftor. We show that ivacaftor reduces the efficacy of Trikafta in human F508del airway epithelial cells and suggest that a different potentiator might improve the therapeutic efficacy in CF.

Contributorship

FB designed the experiments, analyzed the data and contributed reagents/materials/analysis tools. FB performed Ussing chamber experiments. FB and TC performed and analyzed patch clamp experiments. AB designed Nanion's protocols and established BHK stably expressing F508del-CFTR cells. SM did all cell cultures. SM and ML performed and analyzed Western blot experiments. AC performed and analyzed confocal imaging and immunolocalization experiments. CC and ES collected and provided human airway epithelial cells. FB, AC and ML wrote and edited the manuscript.

Abstract

Trikafta, currently the leading therapeutic in Cystic Fibrosis (CF), has demonstrated a real clinical benefit. This treatment is the triple combination therapy of two folding correctors elexacaftor/tezacaftor (VX445/VX661) plus the gating potentiator ivacaftor (VX770). In this study, our aim was to compare the properties of F508del-CFTR in cells treated with either lumacaftor (VX809), tezacaftor, elexacaftor, elexacaftor/tezacaftor with or without ivacaftor. We studied F508del-CFTR function, maturation and membrane localization by Ussing chamber and whole-cell patch clamp recordings, Western blot and immunolocalization experiments. With human primary airway epithelial cells and the cell lines CFBE and BHK expressing F508del, we found that, whereas the combination elexacaftor/tezacaftor/ivacaftor was efficient in rescuing F508del-CFTR abnormal maturation, apical membrane location and function, the presence of ivacaftor limits these effects. The basal F508del-CFTR short-circuit current was significantly increased by elexacaftor/tezacaftor/ivacaftor and elexacaftor/tezacaftor compared to other correctors and non-treated cells, an effect dependent on ivacaftor and cAMP. These results suggest that the level of the basal F508del-CFTR current might be a marker for correction efficacy in CF cells. When cells were treated with ivacaftor combined to any correctors, the F508del-CFTR current was unresponsive to the subsequently acute addition of ivacaftor unlike the CFTR potentiators genistein and Cact-A1 which increased elexacaftor/tezacaftor/ivacaftor and elexacaftor/tezacaftor-corrected F508del-CFTR currents. These findings show that ivacaftor reduces the correction efficacy of Trikafta. Thus, combining elexacaftor/tezacaftor with a different potentiator might improve the therapeutic efficacy for treating CF patients.

Introduction

Cystic fibrosis (CF; MIM#219700), one of the most common, lethal and autosomal recessive disease is caused by mutations in the *CFTR* gene (MIM#602421) encoding the anion channel CFTR (Cystic Fibrosis Transmembrane Conductance Regulator). CFTR is a key player in transepithelial fluid secretion [1]. A defect in its expression, apical location or function, results in CF to a multisystem pathology with severe pulmonary (accumulation of thick, sticky mucus in the bronchi of the lungs) and digestive impairments (loss of exocrine pancreatic function, impaired intestinal absorption) [1]. The most common CF mutation, a deletion of phenylalanine at position 508 (F508del), is a class-2 mutation exhibiting inefficient maturation and reduced plasma membrane expression of the protein [2-4]. F508del-CFTR also exhibits a gating defect [5], a reduced stability at the plasma membrane [6,7] and thermal instability at physiological temperature [8,9]. This mutation is present in about 85% and 81% of the individuals in the US [10] and in Europe [11] respectively. Overall, CF affects over 31,000 people in the US [10] and almost 50,000 people in 38 European countries [11].

It is now agreed that these F508del-defects cannot be addressed by a classical monotherapy but by combination of modulators addressing single defects (i.e. correctors and potentiators acting respectively on protein maturation/folding and channel function) [12, 13]. Applying single F508del-corrector such as VX809 (lumacaftor) [14] or VX661 (tezacaftor) has little efficiency, while combining them to the gating potentiator VX770 (ivacaftor) [15-17] leading respectively to the marketed medicaments Orkambi™ and Symdeko™, improve function despite a modest clinical benefit [18-21] possibly due to interference between corrector and potentiator compounds [22-24].

To overcome the limited efficacy of first-generation correctors, novel second-generation correctors were further developed (Table 1). This strategy gave birth to the triple combination elexacaftor/tezacaftor/ivacaftor (Trikafta™ in USA/Kaftrio™ in EU) approved for treatment of CF patients aged 12 years and older with at least one F508del mutation in the CFTR protein [25-27]. Phase 3 clinical trials with Trikafta were conclusive, describing a better gain in lung functions (augmented percent predicted forced expiratory in 1 second or ppFEV and reduction in lung exacerbation) as compared to Orkambi and Symdeko (Table 1) and improvement in the quality of life of patients [25-27]. Moreover, Trikafta was also effective on rare misfolding mutants of CFTR such as S13F, R31C, G85E, E92K, V520F, M1101K and N1303K [28, 29]. This suggests that Trikafta/Kaftrio might be prescribed to CF patients with at least one copy of the *CFTR* gene with one class 2 misfolding mutation.

Because few reports are available dissecting the functional recovery of F508del by Trikafta in airway epithelial cells, our aim was here to study and compare in more detail the effects of the components of Trikafta with or without ivacaftor on the function, maturation and pharmacological properties of F508del-CFTR in human airway epithelial cells.

Materials and Methods

Cell culture

Human airway epithelial (HAE) cells were obtained from the department of thoracic surgery and lung transplantation of the Foch hospital (Suresnes, France) from explanted CF lungs at the time of patient's transplantation [30]. Human tissues from three F508del/F508del donors were collected and used according to the French law, with the informed consent of patients and through the authorization of Biological Collection n°DC-2012-1583 obtained from the French

Ministry of Higher Education and Research, and with the approval n°21-775 of IRB 00003888. Airways were dissected and epithelial cells obtained after overnight enzymatic dissociation using 0.5 mg/ml pronase E (Sigma Aldrich, USA). Primary HAE cells were seeded on type IV collagen-coated dishes and cultured in Pneumacult™-Ex medium (StemCell Technologies, France) supplemented with tobramycin (80 $\mu g.mL^{-1}$), ceftazidime (100 $\mu g.mL^{-1}$), vancomycin (100 $\mu g.mL^{-1}$), amphotericin B (0.25 $\mu g.mL^{-1}$), penicillin (100 units. mL^{-1}) and streptomycin (100 $\mu g.mL^{-1}$) (Sigma Aldrich, USA).

The human bronchial epithelial cell lines non-CF (CFBE41o$^-$ WT-CFTR cells) and CF (CFBE41o$^-$ F508del-CFTR cells), provided by Dr. D. Gruenert (Univ. California San Francisco, USA), were grown at 37°C in 5% CO_2 - 95% air and media were replaced every 2 days [30]. These cell lines were grown in Eagle's Minimum Essential Medium (EMEM) containing non-essential amino acids (Gibco, USA) supplemented with 10 % fetal bovine serum (FBS) (Eurobio, France), 2 mM L-glutamine, 50 units.mL^{-1}, penicillin, 50 $\mu g.mL^{-1}$ of streptomycin (Sigma Aldrich, USA) and were selected using 5 $\mu g.mL^{-1}$ puromycin (Gibco, USA). F508del-CFTR proteins were restored to the plasma membrane by incubating cells with various combinations of VX445, VX661, VX809, VX770 (see text for details) during 24h, prior to experiments.

The Baby Hamster Kidney (BHK) cell line was cultured in DMEM/F12 medium supplemented with 5% FBS and 1% Penicillin/Streptomycin. To study F508del-CFTR chloride currents by patch clamp and protein maturation by Western blot, BHK were stably transfected with pNUT-F508del- or wild-type-CFTR plasmids using JetPeI reagent (Polyplus, Illkirch, France) according to the manufacturer's instructions. Clones were selected by addition of methotrexate (500 µM) and CFTR expression validated by immunoblotting.

Modulator treatment

F508del-CFTR expressing cells used in the present study were treated by modulators 24h prior to the experiments. The following modulators (Fig.S1A) were used: VX809 (lumacaftor, 3 µM), VX661 (tezacaftor, 18 µM), VX445 (elexacaftor, 3 µM), VX809/VX770 (Orkambi, 3 µM and 1 µM, respectively), VX661/VX770 (Symdeko, 18 µM and 1 µM, respectively), VX445/VX661 (3 µM and 18 µM, respectively) and Trikafta composed of VX661 (18 µM) plus VX445 (3 µM) plus VX770 (1 µM). In our study, we selected the concentrations used by Keating et al. [25] describing the *in vitro* effect of these compounds on CF airway epithelial cells; VX661 at the concentration of 18 µM, VX445 at 3 µM and VX770 at 1 µM. In some experiments we also used VX809 (3 µM) instead of VX661 in the triple combination of VX809/VX445/VX770.

Short-circuit current measurements

HAE cells from distinct F508del/F508del donors were seeded at a density of $0.1x10^6$ cells on type IV collagen-coated Snapwell permeable inserts (Corning Corp., USA) as described [30]. They were cultured in liquid/liquid conditions in Pneumacult™-Ex medium for 5-7 days until confluence was reached and then at air/liquid interface for 21 to 28 days. The culture medium was composed of 1:1 DMEM/F12 (Gibco, USA) and BEGM (Lonza, Switzerland) with the Lonza supplements for hEGF, epinephrine, BPE, hydrocortisone, insulin, triiodothyronine and transferrin. The culture medium was finally supplemented with 50 units.mL^{-1} penicillin (Sigma Aldrich), 50 µg.mL^{-1} streptomycin (Sigma Aldrich, USA), 0.1 nM retinoic acid (Sigma Aldrich) and 1.5 µg.mL^{-1} bovine serum albumin (Sigma Aldrich, USA). The CFBE epithelial cells were seeded at a density of $0.5x10^6$ cells on Snapwell permeable inserts (Corning Corp., USA) coated

with 5 μg.cm^{-2} human fibronectin (Sigma Aldrich, USA) as described in [30]. After 2 days at liquid/liquid interface, cells were cultured at air/liquid interface. The transepithelial resistance of our HAE cultures and CFBE F508del reached a minimum of ~1100-1900 Ω.cm^{-2} and ~400-500 Ω.cm^{-2}, respectively, as measured with a Millicell-ERS voltmeter-ohmmeter (Merck Millipore, USA) the day of Ussing experiment.

Inserts containing pseudo-epithelia were then mounted in an EM-CSYS-6 non-perfused Ussing chamber system (Physiologic Instruments Inc., USA) composed of two hemi-chambers, each containing a different solution. Asymmetric solutions were used, creating a basal to apical Cl^- gradient to enhance Cl^- currents detection. Their compositions were (in mM): 1.2 NaCl, 115 Na-Gluconate, 25 $NaHCO_3$, 1.2 $MgCl_2$, 4 $CaCl_2$, 2.4 KH_2PO_4, 1.24 K_2HPO_4, 10 mannitol (pH 7.4) for apical solution and 115 NaCl, 25 $NaHCO_3$, 1.2 $MgCl_2$, 1.2 $CaCl_2$, 2.4 KH_2PO_4, 1.24 K_2HPO_4, 10 glucose (pH 7.4) for basal solution. Apical and basal solutions were maintained at 37°C (controlled before and after each experiment) and gassed with 95% O_2-5% CO_2. Transepithelial potential difference and short-circuit currents were measured/injected through 3 M KCl filled Ag/AgCl electrodes connected to a VCC MC2 voltage/current clamp (Physiologic Instruments Inc., USA). Visualization and recording of the current injected by the system to short-circuit pseudo-epithelia (clamp at 0 mV) was visualized and recorded at a frequency of 0.1 Hz on a personal computer using Acquire and Analyze hardware and software (Physiologic Instruments Inc., USA). Transepithelial potential difference were corrected for the junction potential between apical and basal solutions and for empty insert resistance. Since the polarity of Isc was referred to the basal side of the pseudo-epithelium and a gain of -10 was applied, an apical anion secretion was indicated by an increase in Isc.

Figure S1B shows the assay protocol for the activation and inhibition of F508del-CFTR mediated chloride currents recorded in our cell models. Pharmacological reagents were added to the apical bathing solution. In all experiments, the transepithelial F508del-CFTR current (short circuit current noted Isc) was assessed after blocking sodium currents by amiloride (100 μM) and 15 min later, CFTR activation was induced by various agonists (forskolin, VX770, Genistein [31] and Cact-A1 [32]). To inhibit CFTR specific Cl^- secretion, we added either CFTR-inh172 (10 μM) [33] or GlyH-101 (15 μM) [34]. Adding UTP (100 μM, not illustrated) after CFTR inhibition was used to control calcium activated chloride channels (CaCC) activity and integrity of the cells at the end of experiments. Figure S1C illustrates our analysis of Isc. We recorded the basal current obtained after stability of the Isc, that is reached 5-15 min after adding amiloride. After 15 minutes we measured the forskolin- and/or potentiator-dependent delta Isc and finally the delta Isc after blocking CFTR.

Patch-clamp experiments

The BHK cell line stably expressing F508del-CFTR was used for the patch-clamp experiments, essentially as in [35]. Automated whole-cell patch clamp was performed on the 8 channel Patchliner NPC-16 workstation (Nanion Technologies GmbH, Munich, Germany), which was coupled to two QuadroEPC-10 amplifiers (HEKA Elektronik GmbH, Germany). Our procedures followed Nanion's standards and used Nanion's high resistance chips (resistances of 3-3.5 MΩ). To record CFTR currents, pulses from the holding potential of −40 mV to test potentials between −80 and +80 mV in 20 mV increments were used. Results were expressed as the current density/voltage [35]. The external bath solution contained (in mM): 145 NMDG, 145 HCl, 10 TES, 5 $BaCl_2$, 2 $CaCl_2$, 2 $MgCl_2$ (titrated with NMDG to pH7.4). The osmolarity of the bath

solution was 300±10 mOsmol. The internal solution contained (in mM): 105 NMDG, 30 H_2SO_4, 20 HCl, 10 TES, 10 EGTA, 4 $MgCl_2$ and 3 MgATP titrated to pH 7.2 with HCl. Osmolarity of the pipette solution was 285±5 mOsmol. A theoretical E_{Cl-} of −44 mV was determined with the Nernst equation. Recordings were performed at room temperature (20-25°C). Results were analyzed with Patch MasterPro software (HEKA).

Western blotting

To determine CFTR expression, CFBE F508del-CFTR, CFBE wild-type CFTR, BHK cells stably expressing F508del-CFTR or wild-type CFTR were lysed using a lysis buffer containing 10 mM Tris HCl, 1% Nonidet P-40, 0.5% sodium deoxycholate, 1 mM Pefabloc® SC (Sigma Aldrich, USA) and the protease inhibitors cocktail complete™ (Roche, Germany). Next, protein extracts were quantified using BCA kit (Pierce™) and 50 µg of protein samples were separated on SDS-PAGE (7%) and transferred to a nitrocellulose membrane. Membrane was then subjected to Western blotting using a mouse anti-CFTR antibody (MAB3480, a.a 1370-1380, clone M3A7, 1:1000; Merck Millipore, USA) [36] and a mouse anti-Na^+/K^+ ATPase (1:1000; SantaCruz biotechnology, USA). Horseradish peroxidase-conjugated sheep anti-mouse antibody (1:5000; Amersham, GE Healthcare, UK) was used as secondary antibody, and proteins were detected using enhanced chemiluminescence (Immobilon, Merck Millipore, France). Images were obtained using the GeneGnome Imager (SynGene Ozyme, France) and analyzed for densitometry with the Genetools software (SynGene Ozyme, France). The intensity of the bands was normalized to the loading control, the Na^+/K^+ ATPase protein and CFTR maturation status was estimated by the band B/ (band B + band C) ratio. The Rainbow™ Molecular Weight

Markers (Amersham, USA) have been used for identification of proteins on SDS-polyacrylamide gels.

Immunofluorescence

At the end of the Ussing experiments, CFBE cells were directly fixed in the insert using 3% paraformaldehyde for 10 min, and conserved at 4°C until immunostaining. Then, cells were permeabilized for 5 min with 0.1% Triton X-100 diluted in PBS and incubated with a mouse anti-human CFTR antibody (MAB25031, aa 1377-1480, Clone # 24-1, 1:400, Bio-Techne, USA) blocked with 1% BSA (Sigma Aldrich, USA) for 2 hours at room temperature. After three 5-min washes, cells were incubated with Alexa Fluor™ 647-conjugated donkey anti-mouse antibody (AF647, 1:200; Invitrogen, USA) for 1 hour and rinsed again 3 times. Immunostaining was followed by 5 min staining of the cell nuclei with Diamidino-phenyl-indole (DAPI, 1:1000, Sigma Aldrich, USA). Each filter was then detached from its insert under binocular loupe with scalpel blade and mounted with mowiol within microscope slide and coverslip (Menzel-Gläser, Sigma Aldrich, USA).

Confocal imaging and analysis

FV3000 confocal microscope (Olympus, France) was used to acquire high resolution 3D images with x60/1.40 Oil objective (UPLXAPOXO). 405 nm and 640 nm laser lines were used for detection of DAPI (Emλ: 430–470 nm) and AlexaFluor 647 (Emλ: 650–750 nm). Z-stack images were acquired with 0.2 stepsize through the entire depth of the sample. Z sections were obtained with Imaris software (Bitplane, Oxford Instrument, Belfast). 3D images were also analyzed with Fiji software. First quantification of CFTR staining was performed on maximum intensity

projection images (MIP). A minimum of 15 regions of interest (ROI) were defined on each field with contrast enhancing if needed (but not applied) in order to identify significant number of cells throughout the image (5 images per condition). Experiment was repeated twice on two different cell cultures. As second analysis, a study of CFTR staining along Z axis was done with the same ROI defined as previously described for quantification. Data were analyzed with excel software. For all the 15 ROIs per image, mean values obtained along Z axis (0.2 µm step) were manually aligned on AF647 peak intensity and mean curve generated for each image. Mean curves of 5 images were then treated in the same manner to align their AF647 peak value and final mean curve was calculated. Values from DAPI channel followed AF647 Z realignment and was treated as AF647 signal to calculate global mean and normalized.

Chemicals

Amiloride, UTP (Uridine 5'-triphosphat), forskolin, genistein, MK571 were from Sigma (Sigma Aldrich, USA). The selective CFTR inhibitors CFTR-$_{inh}$172 and GlyH101 and the CFTR activator Cact-A1 (5-((*Z*)-2-(2-(Allyloxy)phenyl)-1-cyanovinyl)-3-amino-1H-pyrazole-4-carbonitrile, (*Z*)-3-(2-(2-(Allyloxy)phenyl)-1-cyanovinyl)-5-amino-1H-pyrazole-4-carbonitrile) were from Calbiochem (Calbiochem, USA). The following compounds were from Selleckchem (Selleck Chemicals, USA) (IUPAC name): VX445 (elexacaftor), (*N*-(1,3-dimethylpyrazol-4-yl)sulfonyl-6-[3-(3,3,3-trifluoro-2,2-dimethylpropoxy)pyrazol-1-yl]-2-[(4*S*)-2,2,4-trimethylpyrrolidin-1-yl]pyridine-3-carboxamide); VX661 (tezacaftor), (1-(2,2-difluoro-1,3-benzodioxol-5-yl)-*N*-[1-[(2*R*)-2,3-dihydroxypropyl]-6-fluoro-2-(1-hydroxy-2-methylpropan-2-yl)indol-5-yl]cyclopropane-1-carboxamide); VX770 (ivacaftor), (*N*-(2,4-di*tert*-butyl-5-hydroxyphenyl)-4-oxo-1*H*-quinoline-3-carboxamide); VX809 (lumacaftor), (3-[6-[[1-(2,2-

difluoro-1,3-benzodioxol-5-yl)cyclopropanecarbonyl]amino]-3-methylpyridin-2-yl]benzoic acid). Note that VX445 is not chiral purity and thus the manufacturer does not specify enantiomeric VX-445 forms (S, R). Stock solutions of these pharmacological agents were prepared in dimethyl sulfoxide (DMSO) to make a 1000-fold concentrated stock solutions.

Statistical analysis

Data are presented as mean ± SEM of *n* observations. Statistical comparisons were made using non-parametric ($n < 10$) or parametric ($n \geq 10$) tests with a significance level of 0.05. Before using a parametric test, samples were checked for normality using Shapiro-Wilk normality test. Statistical significance was determined with Mann-Whitney test using GraphPad Prism version 6.0 (GraphPad Software, San Diego, CA, USA) software. Differences were considered statistically significant at $P<0.05$. ns, no significant difference; $*P< 0.05$; $**P< 0.01$; $***P< 0.001$ *and* $****P< 0.0001$.

Results

Rescue of F508del-CFTR-dependent transepithelial currents in primary human airway epithelial (HAE) cells by elexacaftor/tezacaftor with and without ivacaftor

We recorded the F508del-CFTR-dependent short circuit currents (Isc) of primary human airway epithelial (HAE) cells from F508del homozygous CF donors to evaluate the correction effect of the components of Trikafta, elexacaftor/tezacaftor/ivacaftor (or VX445/VX661/VX770 hereafter named 3VX) and elexacaftor/tezacaftor (hereafter named 2VX). In these experiments, Isc was first stimulated by forskolin (FSK, 1 µM) and then by VX770 (1 µM) and finally inhibited by CFTRinh172 (10 µM). In control experiments with HAE incubated 24h in DMSO, FSK and

VX770 were not able to increase Isc as shown Fig.1A. On the contrary, with HAE cells treated by either 2VX (Fig.1B) or 3VX (Fig.1C), adding FSK (1 µM) rapidly increased Isc that then stabilized. We observed three differences with HAE cells treated by either 3VX or 2VX. First, the basal Isc level (before adding FSK) was significantly increased in the 3VX experimental condition compared to 2VX (*P<0.001*, Fig.1D). Second, the Isc response to FSK was significantly increased for inserts treated by 3VX *versus* 2VX (*P<0.001*, Fig.1E). Third, the FSK activated Isc could not be further potentiated (*P<0.01*, Fig.1F) by the acute addition of VX770 (see Fig.1B and Fig.1C). However, as also shown Fig.1C, adding a higher concentration of FSK after VX770 further increased Isc for 3VX-treated HAE cells showing that the chloride current was not maximum after VX770. In all experimental conditions, adding CFTRinh172 (10 µM) rapidly inhibited Isc.

The correctors elexacaftor and tezacaftor synergistically rescue F508del-CFTR function

In a second series of experiments (Fig.2), we recorded F508del-CFTR Isc for CFBE F508del-CFTR epithelial cells incubated 24h with the individual correctors lumacaftor, tezacaftor, elexacaftor and with the combination of elexacaftor/tezacaftor (2VX) at the concentrations indicated in the method section. In each experiment, Isc was stimulated by FSK (1 µM) and then by VX770 (1 µM) and finally inhibited by CFTRinh172 (10 µM). The Isc recorded with cells treated by elexacaftor alone was significantly increased as compared to lumacaftor or tezacaftor. When we combined elexacaftor and tezacaftor (2VX) we recorded a higher Isc with either FSK or FSK+VX770 (Fig.2A-B), in good agreement with previous reports [25, 28, 29]. Moreover, the values obtained show that the level of currents with the combination 2VX cannot be explained by the simple addition of the individual effects measured with elexacaftor or tezacaftor. Indeed,

if we simply add the maximum Isc value reached after adding FSK+VX770 with cells treated with either elexacaftor (n=5, ΔIsc_{VX445}=31±1.4 µA/cm^2) or tezacaftor (n=11, ΔIsc_{VX661}=7.6±0.75 µA/cm^2), it gives a theoretical value below 40 µA/cm^2 whereas the experimental Isc value recorded with cells treated with elexacaftor/tezacaftor was ΔIsc_{2VX}=69±3.5 µA/cm^2 (n=14), indicating that elexacaftor and tezacaftor act synergistically and not additively to rescue F508del function (Fig.2B). This is also the case with FSK alone (ΔIsc_{VX661}=3.3±0.3 µA/cm^2, n=12; ΔIsc_{VX445}=7.6±0.4 µA/cm^2, n=6; theoretical Isc_{2VX} ~11 µA/cm^2; experimental ΔIsc_{2VX}=40±2.8 µA/cm^2 (n=14, *P<0.0001* compared to Isc_{VX445}). This synergy has also been reported by previous reports [25,28]. Finally, our conclusions are also supported by the data on inhibition of Isc as shown figure 2B. The amplitude of the current blocked by CFTRinh172 was not significantly different when compared to the maximum level of Isc recorded after FSK+VX770.

VX770 is unable to potentiate the elexacaftor/tezacaftor/ivacaftor-corrected F508del current

Because the therapeutic preparation Trikafta/Kaftrio is composed of VX445+VX661+VX770 (3VX), we compared the responses of CFBE F508del-CFTR cells after treatment with the same correctors (as in Fig.2A) supplemented with 1 µM ivacaftor, to mimic Trikafta/Kaftrio. Figures 2C-D show the stimulation of F508del-dependent Isc in these experimental conditions. As for the results presented in figure 2A, we stimulated Isc with FSK (1 µM) and then we added VX770 (1 µM). Firstly, we found a significant difference (*P<0.05*) between the FSK-dependent Isc recorded with cells treated with 3VX (ΔIsc_{3VX}=46.4±1.4 µA/cm^2, n=17, Fig.2D) compared to cells treated with 2VX (ΔIsc_{2VX}=40±2.8 µA/cm^2, n=14, Fig.2B). Secondly, for all the correctors or combination of correctors tested, the FSK activated Isc could not be further potentiated

following the acute addition of VX770 (Fig.2C). The maximum level of correction of 3VX (ΔIsc_{3VX}=46.6±1.3 µA/cm^2, n=17) is significantly difference (*P<0.0001)* compared to 2VX (ΔIsc_{2VX}=69±3.5 µA/cm^2, n=14) when cells were stimulated by FSK (1 µM) and acute-VX770 (1 µM) (Fig.2B, D). We replicated these results with VX770 added acutely at various concentrations. To that end, we treated cells by either 3VX (Fig.S2A) or 2VX (Fig.S2B) and stimulated Isc by FSK (0.1 µM) and increasing concentrations of VX770 from 0.1 to 10 µM. Whereas VX770 (0.1 µM) potently stimulated Isc of cells treated by 2VX as shown in figures 1B and 2A, it is not the case for cells treated by Trikafta as shown in figures 1C and 2C, even at high concentrations (Fig. S2A). VX770 is also able to stimulate Isc at lower concentrations of cells treated with 2VX (i.e. 0.01 µM, data not shown) as shown previously [15].

We observed in HAE and CFBE F508del-CFTR cells that the effect of FSK to activate F508del-CFTR was more pronounced when VX770 was present in the treatment mixture. Indeed, our recordings of Isc always show that FSK (at 0.1 or 1 µM) stimulated Isc with a higher amplitude for cells treated by 3VX than by 2VX (Fig.1, Fig.2 and Fig.S2). We thus compared the effect of various concentrations of FSK on Isc for both conditions of treatment and found that at any FSK concentrations tested, the Isc amplitude was increased for 3VX-treated cells (Fig.S2C), i.e. most probably due to the presence of VX770. However, the EC_{50} values calculated for FSK (Fig.S2C) were comparable for cells treated with either 3VX (~153 nM) or 2VX (~183 nM) suggesting that FSK has a similar potency in stimulating Isc but an increased efficacy when VX770 is present together with the correctors elexacaftor/tezacaftor. Keating et al [25] also showed that the Isc stimulated by FSK (10 µM) in human bronchial epithelial cells treated by Trikafta was increased compared to elexacaftor/tezacaftor treatment.

To confirm the successful functional rescue of F508del-CFTR by elexacaftor/tezacaftor/ivacaftor, as measured in Ussing experiments with human airway epithelial cells, we recorded F508del-CFTR whole-cell chloride currents in BHK cells stably expressing F508del-CFTR. F508del-CFTR BHK cells were treated by 3VX (Trikafta; n=15) and DMSO (n=14) as control. Figure S3 shows representative whole-cell current traces (A) and corresponding current density/V curves (B, C) from experiments in basal, after addition of FSK (10 µM) + GST (30 µM) and following addition of CFTRinh172 (10 µM). FSK+GST stimulated a chloride current only in 3VX-treated BHK cells (Fig.S3A, C). The current reversed at -40mV, close to the theoretical reversal potential for a chloride current in our experimental conditions (see methods). Finally, adding CFTRinh172 (10 µM) inhibited the stimulated currents. These results show that the triple combination of Trikafta, elexacaftor/tezacaftor/ivacaftor, also restores F508del-CFTR function in the non-human BHK cell expressing F508del-CFTR.

F508del-CFTR maturation and apical staining are reduced by VX770

To begin to understand why it seems to be better to add VX770 in a second time after elexacaftor/tezacaftor, we were interested by the impact of VX-770 on CFTR protein expression. In fact, it has been reported that ivacaftor destabilizes F508del-CFTR [22,23]. We thus performed Western blot and immunofluorescence analysis with CFBE F508del cells treated by correctors with or without ivacaftor. Figure 3 shows results of Western blot experiments (n=6) on cells either cultured on insert analyzed after measuring Isc with Ussing experiments (Fig.3A) or on plastic dish (Fig.3B). The amount of mature F508del proteins (band C) was significantly increased for CFBE F508del-CFTR cells treated by tezacaftor, elexacaftor, elexacaftor/tezacaftor and elexacaftor/tezacaftor/ivacaftor compared to non-treated cells (Fig.3C). In addition, the

amount of band C of F508del-CFTR was significantly decreased in cells treated by 3VX regarding cells treated by 2VX (Fig.3C). Comparable results were obtained for BHK cells expressing F508del-CFTR. The level of mature F508del proteins (band C) was also increased with 2VX or 3VX treatment (Fig.S3D).

Destabilization of F508del-CFTR by VX770 was also studied by F508del-CFTR immunostaining. Figure 4 presents representative confocal images showing levels of CFTR immunofluorescent staining after 24h-incubation with DMSO, elexacaftor/tezacaftor (2VX) and elexacaftor/tezacaftor/ivacaftor (3VX) (Fig.4A) and representative Z section of 3D confocal images showing apical localization of CFTR staining along thickness of 3D culture in these experimental conditions (Fig.4B). We quantified the mean intensity of fluorescence measured from Z maximum intensity projection images (Fig.4C) and show the reduced intensity of CFTR immunofluorescent staining after 3VX compared to 2VX *($P<0.001$)*. Although we cannot strictly correlate our results obtained by Western blot, Ussing chamber and immunolocalization, these observations qualitatively confirmed that ivacaftor reduces the correction efficacy of Trikafta as shown earlier by others for VX809 (lumacaftor) and VX661 (tezacaftor) [22, 23].

The basal Isc current measured before stimulation as a marker of F508del rescue

During analysis of the Ussing chamber recordings after the various treatments shown in figures 1 and 2, we observed that the basal level of Isc was dependent on the nature of the correction. The value of basal Isc was quantified after amiloride and before stimulation by FSK. In particular with the triple combination elexacaftor/tezacaftor/ivacaftor, we systematically recorded a higher basal Isc compared to other treatments (Fig. 1D and Fig. 2C). With CFBE F508del cells, we determined the basal Isc for all experiments and reported the results in figure 5. For cells treated

by only one corrector, either lumacaftor (VX809, n=7), tezacaftor (VX661, n=10) or elexacaftor (VX445, n=14), the basal Isc was not significantly different compared to DMSO (n=5) and non-treated cells (noted NT, n=15, Fig.5A). The value of basal Isc was also similar for cells treated by one corrector associated to the potentiator VX770 that is either the components of Orkambi (i.e. lumacaftor/ivacaftor; Isc=6.4±0.8 µA/cm^2, n=6) or of Symdeko (i.e. tezacaftor/ivacaftor; Isc_{basal}=5±0.5 µA/cm^2, n=10, Fig.5B). However, the basal Isc value was significantly increased if ivacaftor is associated to elexacaftor treatment (Isc_{basal}=12±1.1 µA/cm^2, n=10, Fig.5B). In the case of the association of two correctors, the basal Isc with elexacaftor/tezacaftor was Isc_{basal}=8±0.5 µA/cm^2 (n=48) and increases to Isc_{basal}=17±0.4 µA/cm^2 if it is associated to the potentiator VX770 (n=68, Fig.5C). The basal Isc was comparable when tezacaftor was substituted by lumacaftor (Isc_{basal}=19±1.6 µA/cm^2, n=4, Fig.5C). The substitution of VX661 by VX809 in the triple combination of Trikafta, neither modify the FSK-stimulated Isc (VX809: ΔIsc=49±2.7 µA/cm^2, n=4, 1 µM FSK) nor the CFTRinh172-dependent Isc (VX809: ΔIsc=50±1.1 µA/cm^2, n=4). Then, to confirm that the basal current was due to CFTR activity, we added the CFTR inhibitor directly on the basal current. An example is shown figure 5D. In these paired experiments we treated cells by elexacaftor/tezacaftor/ivacaftor and added GlyH101 (15 µM) with or without FSK (10 µM) as indicated on the tracings. After GlyH101, both inhibited currents reached a comparable level. Thus, the inhibited Isc current represents the sum of the basal activity of CFTR plus the FSK-activated CFTR activity. Therefore, treating cells with Trikafta, most probably due to the presence of the CFTR potentiator ivacaftor, results in the basal cAMP activation of F508del-CFTR in the absence of any exogenous addition of cAMP agonists. To further study this, in the next experiments we used MK571 an inhibitor of the multidrug resistance protein 4 (MRP4/ABCC4) [37] that is expressed in airway epithelial cells

[38, 39]. Inhibition of MRP4 by MK571 was shown to prevent cAMP efflux within cellular microdomains containing MRP4 and CFTR thereby augmenting phosphorylation of CFTR [37-39]. With CFBE F508del cells treated by elexacaftor/tezacaftor/ivacaftor (Fig. 5E, F) and elexacaftor/tezacaftor (Fig.5G, H), a preincubation with MK571 (20 µM) for 20 min in the apical chamber induced a further increase of basal Isc (Isc_{basal}=29±1.6 µA/cm^2 and 11±1.7 µA/cm^2, respectively, Fig.5C). Representative recordings are shown figures 5E-H. Addition of the CFTR inhibitors GlyH101 (15 µM) or CFTRInh172 (10 µM) inhibited Isc in absence of additional stimulation (Fig.5E, G) or after 1 µM FSK (Fig.5F, H). In addition, we observed that the effect of MK571 was significantly reduced *(P<0.01)* in cells treated by elexacaftor/tezacaftor compared to cells treated by elexacaftor/tezacaftor/ivacaftor (Fig.5C).

Potentiation of Trikafta-corrected F508del-CFTR function

A striking difference observed in both HAE (Fig.1) or CFBE F508del cells (Fig.2) treated by elexacaftor/tezacaftor/ivacaftor or by only the two correctors elexacaftor/tezacaftor (i.e. without ivacaftor) is that adding VX770 cannot further increased Isc. Of note, the prescription of Trikafta to CF patients consists of a first tablet with the triple combination elexacaftor/tezacaftor/ivacaftor and a second tablet with only ivacaftor. Although our *in vitro* analysis of the effect of the components of Trikafta cannot be strictly compared to an *in vivo* exposure of CF patients to Trikafta, we conducted additional experiments to study this difference in more details. To that end, we used elexacaftor/tezacaftor/ivacaftor-treated cells stimulated by 0.1 µM FSK (corresponding to the calculated EC_{50} value as shown Fig.S2C). Acute addition of VX770 (1 µM) before (Fig.6A) or after FSK at different concentrations (Fig.6B, C) failed to increase Isc. To evaluate whether the amplitude of the current reached after FSK+VX770 was

maximal, we added 1 µM FSK (corresponding to the saturating concentration Fig.S2C) after VX770. The addition of 1 µM FSK after VX770 increased Isc (Fig.6A-C), which was inhibited by CFTRinh172. Then, we evaluated the effect of VX770 on cells treated by elexacaftor/tezacaftor. As expected, VX770 (1 µM) was able to stimulate Isc before (Fig.6D) or after FSK (Fig.6E, F) and was inhibited by CFTRinh172. However, VX770-dependent Isc was not maximum because it could be further potentiated by FSK (0.1-1 µM) as shown in figure 6D-F. The Isc presented in Figures 6A and 6D are summarized in Figure 6G. Figure 6H shows results when high concentration of FSK (10 µM) was added before adding VX770 (1µM) for cells treated by either 3VX or 2VX.

Our next question was to determine whether a different potentiator, instead of VX770, would be able to potentiate FSK-activated Isc in Trikafta-treated cells. We thus conducted experiments with the two potentiators, genistein [31] and Cact-A1 [32] and compared their effects with cells treated by either elexacaftor/tezacaftor/ivacaftor (Fig.7A) or elexacaftor/tezacaftor (Fig.7B). We first used low concentration of FSK (0.01 µM) to pre-stimulate Isc and second added genistein (30 µM) or Cact-A1 (30 µM) and finally added saturating FSK (1 µM). Contrary to VX770, both potentiators significantly potentiated the FSK-dependent Isc (Fig.7A, B). The effect of saturating concentration of FSK was however very small compared to the experiments using VX770 (see Fig.6C, F and Fig.7A, B). Since VX770 binds within the transmembrane region of CFTR protein [40], it might prevents the action of different potentiators. Thus, we recorded Isc with CFBE F508del cells treated by either elexacaftor/tezacaftor/ivacaftor (Fig.8A, C) or elexacaftor/tezacaftor (Fig.8B, C) stimulated by genistein after VX770. We also obtained comparable results with F508del-HAE cells treated by either elexacaftor/tezacaftor/ivacaftor (Fig.8D, F) or elexacaftor/tezacaftor (Fig.8E, F) stimulated

by genistein after VX770. In both cell models, these results show that genistein is able to potentiate Isc despite the presence of VX770.

Discussion

The novel medicament for CF patients, Trikafta/Kaftrio (Vertex Pharmaceuticals, USA), is composed of two folding correctors, elexacaftor and tezacaftor and one gating potentiator, ivacaftor. The results of Phase 3 clinical trials demonstrated a significant gain in lung functions with Trikafta as compared to Orkambi and Symdeko (Table 1) [25-27, 41]. Trikafta is indicated for CF patients of 12 years of age and older who have at least one F508del mutation, or at least one other mutation in the CF gene that is responsive to Trikafta (i.e. 177 other approved mutations), regardless of their second mutation type [41]. Although the molecular mechanism of action of these modulators remains unknown, Trikafta might help F508del-CFTR to fold properly to be relocated to the apical plasma membrane of epithelial cells instead of being addressed to the intracellular degradation pathway. Then, the corrected F508del-defective CFTR protein functions more efficiently at the apical membrane of airway epithelial cells [25-29]. In a recent study, Lukacs and colleagues [28] showed that VX445 synergistically restores F508del-CFTR processing in combination with correctors of type I (such as VX661, VX809, ABBV-2222 and FDL169) or II (the compound 3151, [42]). These correctors target the NBD1-MSD interface and NBD2, respectively. These authors proposed that VX445 is a type III corrector stabilizing NBD1 [28, 42]. This is consistent with our results showing synergy between VX445 and VX661 and also with results from experiments in which we substituted VX661 by VX809 (two type I correctors) in the triple combination of Trikafta, and observed no significant differences in the values of ΔIsc. Another recent investigation on double corrector treatment [43] showed that

VX445 elicits a large rescue of F508del-CFTR function as we observed here. However, after analysis of ubiquitylation, resistance to thermoaggregation, protein half-life, and subcellular localization authors concluded that VX445 plus a type I corrector (VX661 or VX809) did not fully normalize F508del-CFTR behavior.

We have explored in that study the effect of the three components of Trikafta (i.e. elexacaftor/tezacaftor/ivacaftor) either alone or in combination and found that in the absence of the potentiator ivacaftor, the order of potency to rescue F508del-CFTR function was lumacaftor ~ tezacaftor << elexacaftor << elexacaftor/tezacaftor, the two folding correctors elexacaftor and tezacaftor acting synergistically [25, 28]. In the presence of the potentiator ivacaftor, we found differences in the order of potency for the ability to rescue F508del function as determined by the amplitude of the FSK-dependent Isc. In that case, Trikafta was the most potent treatment: Orkambi ~ Symdeko << elexacaftor/ivacaftor << Trikafta. On the other hand, we found that the order of potency to rescue the mature form of F508del proteins (form C) was tezacaftor << elexacaftor ~ elexacaftor/tezacaftor/ivacaftor < elexacaftor/tezacaftor. A similar result was reported by Keating et al [25].

However, for the triple combination Trikafta (this study and [25, 28]), like for the double combinations Orkambi and Symdeko [22, 23], the gating potentiator ivacaftor reduced the correction efficacy of these treatments as observed for F508del-CFTR localization, maturation and function in airway epithelial cells. As reported earlier with lumacaftor and tezacaftor [22-24], this effect is due to the progressive loss of CFTR at the plasma membrane following its activation. An effect that might also be related to the lipophilicity of ivacaftor at the origin of nonspecific effects on the lipid bilayer [44]. This membrane effect may account

for the destabilizing effect of ivacaftor on lumacaftor-rescued F508del-CFTR as recently shown [44]. Our Western blot and immunolocalization studies of F508del proteins are in good agreement with these observations and therefore confirmed that ivacaftor has also a destabilizing effect on F508del rescued by Trikafta, as shown [25, 28].

A comparison of the basal Isc suggests that the inhibited Isc current represents the sum of the basal activity of CFTR plus the FSK/potentiator-activated CFTR activity (i.e. a+b+c figure S1C). We thus believe that with Trikafta, the basal Isc reflects the fact that F508del-CFTR is not only resident (due to the synergic correcting action of elexacaftor/tezacaftor) but also functional at the plasma membrane of cells (due to the binding of ivacaftor to F508del-CFTR and opening of the channels) under the control of an endogenous cAMP pathway. A raise of the basal and FSK-mediated Isc by MK-571 in elexacaftor/tezacaftor/ivacaftor or elexacaftor/tezacaftor treated cells could occur through induction of local elevations in cytosolic cAMP as suggested by the description of the spatiotemporal coupling between the cAMP transporter MRP4 and CFTR activity in intestinal [37] and airway cells [38, 39]. Therefore, we propose here that the basal Isc, a value generally neglected, could represents a marker of the level of correction of functional F508del-CFTR and could serve as a readthrough to identify synergistic combinations of F508del-CFTR modulators. Our results are also in agreement with those of Keating et al [25] showing that the Isc stimulated by FSK in human airway epithelial cells treated with Trikafta was increased compared to a treatment by elexacaftor/tezacaftor.

We thus believe that the level of stimulation of CFTR-dependent Isc is underestimated when ivacaftor is used as potentiator. Despite the fact that ivacaftor was very potent to acutely potentiate the rescued F508del-CFTR-dependent Isc when cells were treated with elexacaftor/tezacaftor, the potentiator was unable to activate CFTR-Isc in Trikafta-treated cells.

At least two studies might explain our results. Firstly, recent evidences from experiments of cryoelectron microscopy showed structure of human CFTR in complex with the two potentiators ivacaftor and GLPG1837 binding to the same site within the transmembrane region of CFTR [40]. Therefore, a direct binding of ivacaftor to F508del might explain why, after 24h incubation, the acute addition of ivacaftor was unable to stimulate CFTR current simply because the binding sites are still occupied. This was not the case for genistein and Cact-A1 that are still able to stimulate the rescued F508del current above the level achieved by FSK and despite the presence of ivacaftor (chronic or acute). The most plausible reason being that ivacaftor and genistein do not compete to the same binding site. Indeed, genistein has been shown to interact with nucleotide binding domains (although no binding has been firmly shown) [45, 46] but not with the transmembrane region of CFTR where ivacaftor binds [40]. Unfortunately, genistein has no clinical benefit on some CFTR variants [47] and therefore cannot replace ivacaftor. Secondly, it has been shown that ivacaftor accumulates in CF-HBE cells to a much greater extent than either lumacaftor or tezacaftor, remaining persistently elevated even after 14 days of washout. CFTR activity peaked at 7 days of treatment but diminished with further ivacaftor accumulation, though remained above baseline even after washout [48].

In conclusion, our study confirms the efficacy of the components of Trikafta to rescue a mature and functional form of F508del-CFTR at the apical plasma membrane of human airway epithelial cells. But we also show that ivacaftor has still a destabilizing effect on rescued-F508del and that despite the potency of ivacaftor, it was not able to further potentiate the function of Trikafta-rescued F508del-CFTR. This is important because ivacaftor also reduces the correction efficacy of lumacaftor [22, 23] and tezacaftor [23]. Our results also showed that ivacaftor does not preclude the use of another potentiator combined to Trikafta. Taken together

with previous reports [13, 16, 22-24], our results thus suggest that we should be able to maximize the correcting effect of Trikafta by using a different potentiator.

Acknowledgements

This study was supported by Vaincre La Mucoviscidose (RF20200502704). TC hold a thesis scholarship from ANRT and ManRos therapeutics *via* CIFRE. AB was a recipient of post-doctoral fellowship from the CF Trust (SRC005). ML hold a postdoctoral fellowship from Vaincre La Mucoviscidose (RF20200502704). This work has benefited from the facilities and expertise of ImageUP platform (University of Poitiers).

Conflict of Interest/Disclosures- The authors declare that they have no conflict of interest.

REFERENCES

1. Rowe SM, Miller S, Sorscher EJ. Cystic Fibrosis. N. Engl. J. Med. 2005; 352: 1992–2001.

2. Cheng SH, Gregory RJ, Marshall J, Paul S, Souza DW, White GA, et al. Defective intracellular transport and processing of CFTR is the molecular basis of most cystic fibrosis. Cell 1990; 63: 827–834.

3. Denning GM, Ostedgaard, LS, Welsh MJ. Abnormal localization of cystic fibrosis transmembrane conductance regulator in primary cultures of cystic fibrosis airway epithelia. J. Cell Biol. 1992; 118: 551-559.

4. Welsh MJ, Smith AE. Molecular mechanisms of CFTR chloride channel dysfunction in cystic fibrosis. Cell. 1993; 73:1251–1254.

5. Dalemans W, Barbry P, Champigny G, Jallat S, Dott K, Dreyer D, et al. Altered chloride ion channel kinetics associated with the delta F508 cystic fibrosis mutation. Nature 1991; 354: 526–528.

6. Lukacs GL, Chang XB, Bear C, Kartner N, Mohamed A, Riordan JR, et al. The delta F508 mutation decreases the stability of cystic fibrosis transmembrane conductance regulator in the plasma membrane. Determination of functional half-lives on transfected cells. J. Biol. Chem. 1993; 268: 21592–8.

7. Okiyoneda T, Barrière H, Bagdány M, Rabeh WM, Du K, Höhfeld J, et al. Peripheral protein quality control removes unfolded CFTR from the plasma membrane. Science 2010; 329: 805-10.

8. Liu X, Dawson DC. Cystic fibrosis transmembrane conductance regulator (CFTR) potentiators protect G551D but not ΔF508 CFTR from thermal instability. Biochemistry. 2014; 53(35): 5613-8.

9. Wang W, Okeyo GO, Tao B, Hong JS, Kirk KL. Thermally Unstable Gating of the Most Common Cystic Fibrosis Mutant Channel (ΔF508): "Rescue" by Suppressor Mutations in Nucleotide Binding Domain 1 and by Constitutive Mutations in the Cytosolic Loops. J. Biol. Chem. 2011; 286: 41937–41948.

10. Cystic Fibrosis Foundation. Patient Registry: 2019 Annual Data Report.

11. European Cystic Fibrosis Society Patient Registry Annual Data Report. 2018, Zolin A, Orenti A, Naehrlich L, Jung A, van Rens J et al, 2020.

12. Veit G, Avramescu RG, Chiang AN, Houck SA, Cai Z, Peters KW, et al. From CFTR biology toward combinatorial pharmacotherapy: expanded classification of cystic fibrosis mutations. Mol. Biol. Cell 2016; 27: 424–433.

13. Okiyoneda T, Veit G, Dekkers JF, Bagdany M, Soya N, Xu H, et al. Mechanism-based corrector combination restores ΔF508-CFTR folding and function. Nat. Chem. Biol. 2013; 9, 444–454.

14. Van Goor F, Hadida S, Grootenhuis PD, et al. Correction of the F508del-CFTR protein processing defect in vitro by the investigational drug VX-809. Proc Natl Acad Sci U S A. 2011; 108(46): 18843-8.

15. Van Goor F, Hadida S, Grootenhuis PD, Burton B, Cao D, Neuberger T, Turnbull A, Singh A, Joubran J, Hazlewood A, et al. Rescue of CF airway epithelial cell function *in vitro* by a CFTR potentiator, VX-770. Proc Natl Acad Sci USA 2009; 106: 18825–30.

16. Dekkers JF, Van Mourik P, Vonk AM, et al. Potentiator synergy in rectal organoids carrying S1251N, G551D, or F508del CFTR mutations. J Cyst Fibros. 2016 Sep;15(5):568-78.

17. Phuan PW, Son J-H, Tan J-A, Li C, et al. Nanomolar-potency 'co-potentiator' therapy for cystic fibrosis caused by a defined subset of minimal function CFTR mutants. Sci Rep. 2019 Nov 27;9(1):17640.

18. Wainwright CE, Elborn JS, Ramsey BW, et al. Lumacaftor-Ivacaftor in Patients with Cystic Fibrosis Homozygous for Phe508del CFTR. N Engl J Med. 2015; 373(3): 220-31.

19. Rehman A, Baloch NU, Janahi IA. Lumacaftor-Ivacaftor in Patients with Cystic Fibrosis Homozygous for Phe508del CFTR. N Engl J Med. 2015; 373(18):1783.

20. Taylor-Cousar JL, Munck A, McKone EF et al. Tezacaftor-Ivacaftor in Patients with Cystic Fibrosis Homozygous for Phe508del. N Engl J Med. 2017; 377(21): 2013–2023.

21. Rowe SM, Daines C, Ringhausen FC et al. Tezacaftor-Ivacaftor in Residual-Function Heterozygotes with Cystic Fibrosis. N Engl J Med. 2017; 377(21): 2024–2035.

22. Cholon DM, Quinney NL, Fulcher ML, Esther CR, Das J, Dokholyan NV, Randell SH, Boucher RC, Gentzsch M. Potentiator ivacaftor abrogates pharmacological correction of ΔF508 CFTR in cystic fibrosis. Sci. Transl. Med. 2014; 6: 246ra96.

23. Veit G, Avramescu RG, Perdomo D, et al. Some gating potentiators, including VX-770, diminish ΔF508-CFTR functional expression. Sci Transl Med. 2014; 6(246): 246ra97.

24. Avramescu RG, Kai Y, Xu H, Bidaud-Meynard A, Schnúr A, Frenkiel S, Matouk E, Veit G, Lukacs GL. Mutation-specific downregulation of CFTR2 variants by gating potentiators. Hum Mol Genet. 2017; 26(24): 4873-4885.

25. Keating D, Marigowda G, Burr L, Daines C, Mall MA, McKone EF, et al. VX-445-Tezacaftor-Ivacaftor in Patients with Cystic Fibrosis and One or Two Phe508del Alleles. N Engl J Med. 2018; 379(17): 1612-1620.

26. Heijerman HGM, McKone EF, Downey DG, Van Braeckel E, Rowe SM, Tullis E, et al. Efficacy and safety of the elexacaftor plus tezacaftor plus ivacaftor combination regimen in people with cystic fibrosis homozygous for the F508del mutation: a double-blind, randomised, phase 3 trial. Lancet. 2019; 394(10212): 1940-1948.

27. Middleton PG, Mall MA, Drevinek P, et al. Elexacaftor-tezacaftor-ivacaftor for cystic fibrosis with a single phe508del allele. N Engl J Med. 2019; 381(19): 1809-1819.

28. Veit G, Roldan A, Hancock MA, Da Fonte DF, Xu H, Hussein M, et al. Allosteric folding correction of F508del and rare CFTR mutants by elexacaftor-tezacaftor-ivacaftor (Trikafta) combination. JCI Insight. 2020;5(18): e139983.

29. Laselva O, Bartlett C, Gunawardena TNA, Ouyang H, Eckford PDW, Moraes TJ, et al. Rescue of multiple class II CFTR mutations by elexacaftor+tezacaftor+ivacaftor mediated in part by the dual activities of Elexacaftor as both corrector and potentiator. Eur Respir J. 2020 Dec 10:2002774. doi: 10.1183/13993003.02774-2020.

30. Froux L, Coraux C, Sage E, Becq F. The Short-term consequences of F508del-CFTR thermal instability on CFTR-dependent transepithelial currents in human airway epithelial cells. Scientific Report. 2019 Sep 24;9(1):13729. doi: 10.1038/s41598-019-50066-7.

31. Hwang T-C, Wang F, Yang IC-H, Reenstra WW. Genistein potentiates wild-type and ΔF508-CFTR channel activity. Am. J. Physiol. - Cell Physiol. 1997; 273 C988-98.

32. Namkung W, Park J, Seo Y, Verkman AS. Novel Amino-Carbonitrile-Pyrazole Identified in a Small Molecule Screen Activates Wild-Type and ΔF508 Cystic Fibrosis Transmembrane Conductance Regulator in the Absence of a cAMP Agonist. Mol Pharmacol 2003; 84: 384–392.

33. Ma T, Thiagarajah JR, Yang H, Sonawane ND, Folli C, Galietta LJV, et al. Thiazolidinone CFTR inhibitor identified by high-throughput screening blocks cholera toxin – induced intestinal fluid secretion. J. Clin. Invest. 2002; 110: 1651–1658.

34. Muanprasat C, Sonawane ND, Salinas D, Taddei A, Galietta LJ, Verkman AS. Discovery of glycine hydrazide pore-occluding CFTR inhibitors: mechanism, structure-activity analysis, and in vivo efficacy. J Gen Physiol. 2004; 124(2): 125-37.

35. Billet A, Froux L, Hanrahan JW, Becq F. Development of Automated Patch Clamp Technique to Investigate CFTR Chloride Channel Function. Front Pharmacol. 2017; 8: 195.

36. Yu W, Chiaw PK, Bear CE. Probing conformational rescue induced by a chemical corrector of F508del-cystic fibrosis transmembrane conductance regulator (CFTR) mutant. J. Biol. Chem. 2011; 286: 24714-24725.

37. Li C, Krishnamurthy PC, Penmatsa H, Marrs KL, Wang XQ, Zaccolo M, et al. Spatiotemporal coupling of cAMP transporter to CFTR chloride channel function in the gut epithelia. Cell. 2007; 131(5): 940-51.

38. Schnúr A, Premchandar A, Bagdany M, Lukacs GL. Phosphorylation-dependent modulation of CFTR macromolecular signalling complex activity by cigarette smoke condensate in airway epithelia. Sci Rep. 2019; 9(1): 12706.

39. Ahmadi S, Bozoky Z, Di Paola M, Xia S, Li C, Wong AP, et al. Phenotypic profiling of CFTR modulators in patient-derived respiratory epithelia. NPJ Genom Med. 2017; 2: 12.

40. Liu F, Zhang Z, Levit A, Levring J, Touhara KK, Shoichet BK, Chen J. Structural identification of a hotspot on CFTR for potentiation. Science. 2019; 364(6446): 1184-88.

41. Cystic Fibrosis Foundation web site (www.cff.org)

42. Veit G, Xu H, Dreano E, Avramescu RG, et al. Structure-guided combination therapy to potently improve the function of mutant CFTRs. Nat Med. 2018 Nov;24(11):1732-1742.

43. Capurro V, Tomati V, Sondo E, et al. Partial Rescue of F508del-CFTR Stability and Trafficking Defects by Double Corrector Treatment. Int J Mol Sci. 2021 May 17;22(10):5262. doi: 10.3390/ijms22105262.

44. Chin S, Hung M, Won A, Wu YS, Ahmadi S, Yang D, et al. Lipophilicity of the Cystic Fibrosis Drug, Ivacaftor (VX-770), and Its Destabilizing Effect on the Major CF-causing Mutation: F508del. Mol Pharmacol. 2018; 94(2): 917-925.

45. Moran O, Galietta LJ, Zegarra-Moran O. Binding site of activators of the cystic fibrosis transmembrane conductance regulator in the nucleotide binding domains. Cell Mol Life Sci. 2005; 62(4): 446-60.

46. Huang SY, Bolser D, Liu HY, Hwang TC, Zou X. Molecular modeling of the heterodimer of human CFTR's nucleotide-binding domains using a protein-protein docking approach. J Mol Graph Model. 2009; 27(7): 822-8.

47. Berkers G, van der Meer R, van Mourik P, Vonk AM, Kruisselbrink E, Suen SW, et al. Clinical effects of the three CFTR potentiator treatments curcumin, genistein and ivacaftor in patients with the CFTR-S1251N gating mutation. J Cyst Fibros. 2020; 19(6): 955-961.

48. Guhr Lee TN, Cholon DM, Quinney NL, Gentzsch M, Esther CR Jr. Accumulation and persistence of ivacaftor in airway epithelia with prolonged treatment. J Cyst Fibros. 2020; 19(5): 746-751.

FIGURE LEGENDS

Figure 1

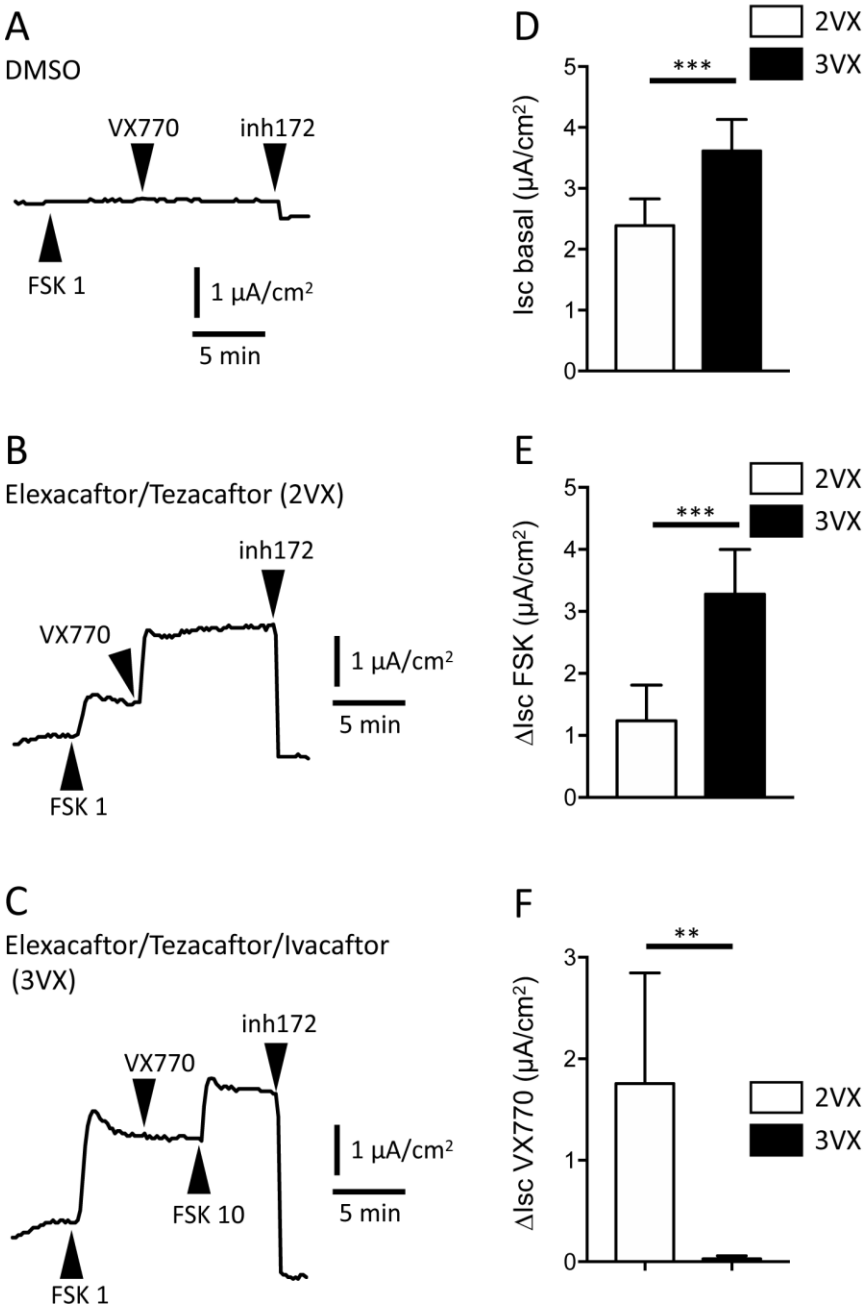

Figure 1: Rescue of F508del-Isc in Human Airway Epithelila cells by elexacaftor/tezacaftor with or without ivacaftor. A-C. Original tracings of Isc as function of time (expressed here and in the following figures as μA/cm^2) for F508del-HAE cells incubated 24h with DMSO (A) elexacaftor/tezacaftor (noted 2VX, B) and the components of Trikafta, i.e. elexacaftor/tezacaftor/ivacaftor (noted 3VX, C). The F508del-CFTR short-circuit current was stimulated by FSK at 1 μM (indicated as FSK 1, first arrow) and then 1 μM VX770 (second arrow) and finally inhibited by 10 μM CFTRinh172 (third arrow). D. Mean ± SEM of Isc basal for HAE cells treated by 2VX (n=6) and 3VX (n=7) as indicated (***$P< 0.001$). E, F. Mean ± SEM of ΔIsc in the presence of FSK (E) and VX770 (F) for HAE cells treated by 2VX (n=6) and 3VX (n=7) as indicated (**$P< 0.01$; ***$P< 0.001$). Here and in the following figures, the concentration of each modulator is given in the method section.

Figure 2

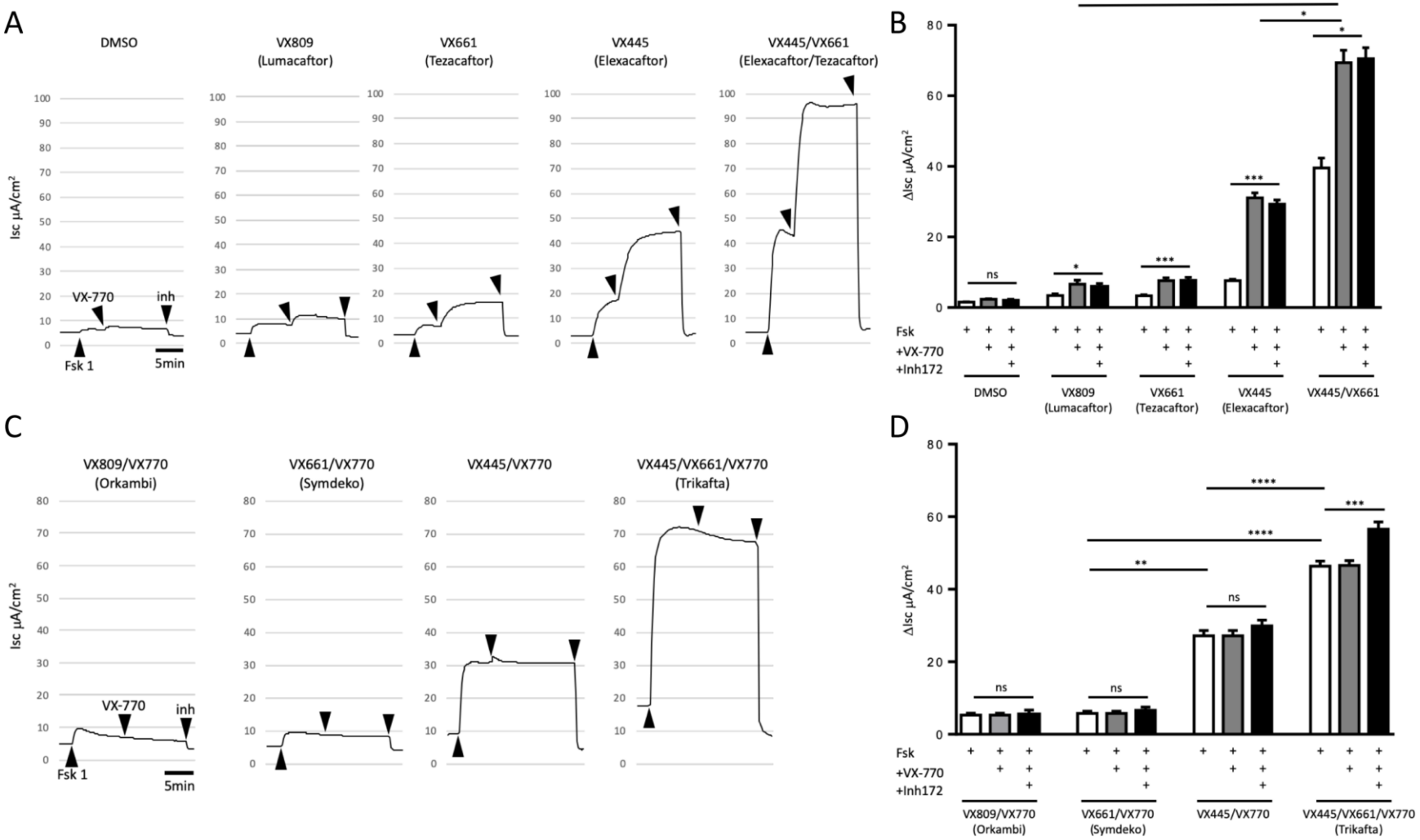
A
DMSO
VX809 (Lumacaftor)
VX661 (Tezacaftor)
VX445 (Elexacaftor)
VX445/VX661 (Elexacaftor/Tezacaftor)
Isc µA/cm²
VX-770
inh
Fsk 1
5min
B
ΔIsc µA/cm²
ns
*
***
**
Fsk
+VX-770
+Inh172
DMSO
VX809 (Lumacaftor)
VX661 (Tezacaftor)
VX445 (Elexacaftor)
VX445/VX661
C
VX809/VX770 (Orkambi)
VX661/VX770 (Symdeko)
VX445/VX770
VX445/VX661/VX770 (Trikafta)
Isc µA/cm²
VX-770
inh
Fsk 1
5min
D
ΔIsc µA/cm²
ns
**
****
***
Fsk
+VX-770
+Inh172
VX809/VX770 (Orkambi)
VX661/VX770 (Symdeko)
VX445/VX770
VX445/VX661/VX770 (Trikafta)

Figure 2: Rescue of F508del-Isc by various correctors in CFBE cells expressing F508del-CFTR. A, C. Original tracings of Isc as function of time for CFBE F508del cells incubated 24h with the corrector indicated at the top of each plot without (A) or with VX770 (C). In A, DMSO was used as control. The Isc CFTR current was stimulated by forskolin at 1 μM (indicated as FSK 1, first arrow) and then 1 μM VX770 (second arrow) and finally inhibited by 10 μM CFTRinh172 (third arrow). B, D. Mean ± SEM of ΔIsc for each condition illustrated in A (n=5-14) and C (n=17). ns, no significant difference; *$P< 0.05$; **$P< 0.01$; ***$P< 0.001$ and ****$P< 0.0001$.

figure 3

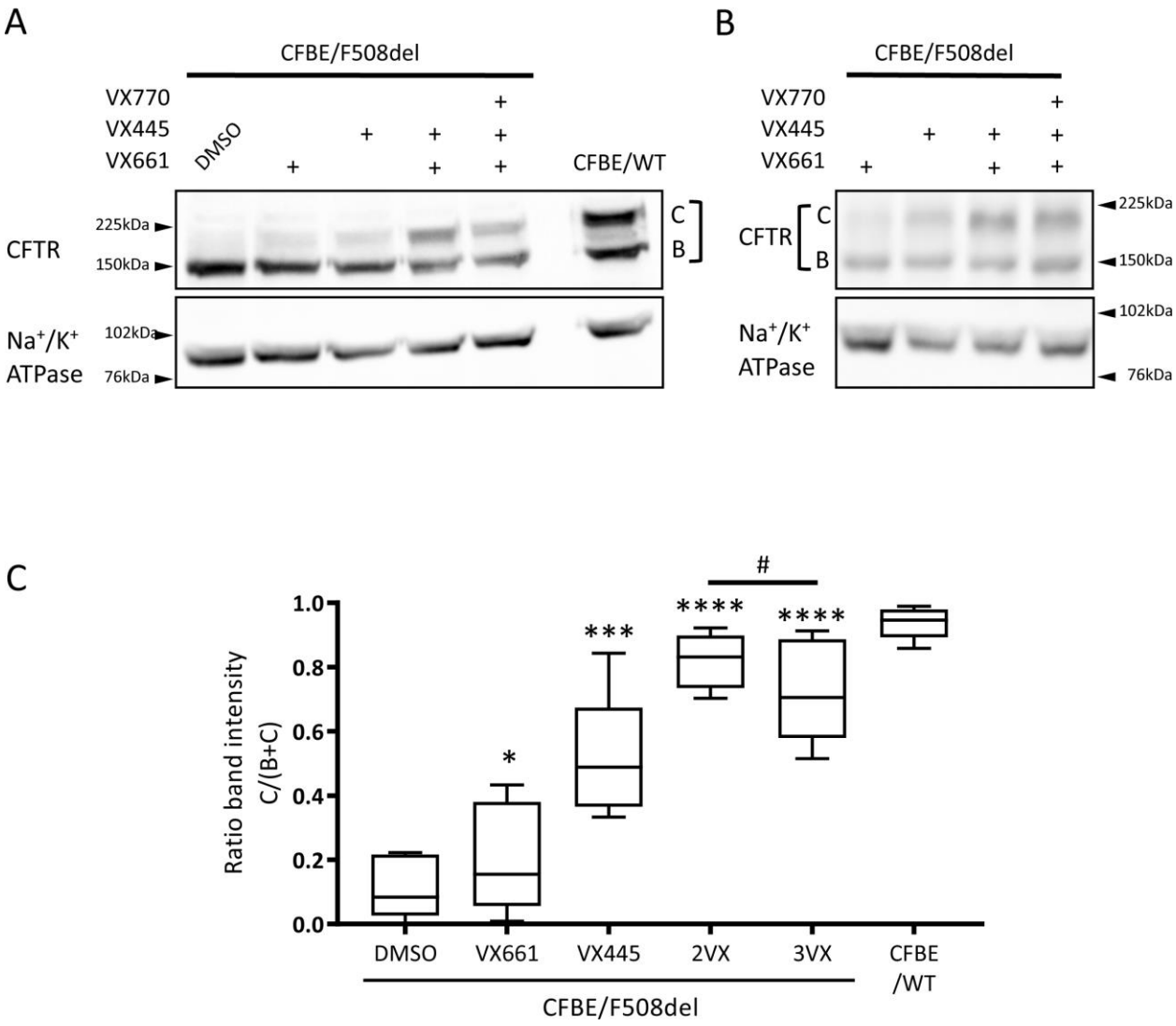

Figure 3. Immunoblots of F508del following treatments with CFTR correctors. A. CFTR expression of the total protein fraction of CFBE F508del cells after 24h-incubation with VX661 (18µM), VX445 (3µM) and VX770 (1µM) or DMSO control as indicated above blot and of CFBE WT cells grown on inserts (representative blot of 6 independent experiments). Equal protein loading was controlled via Na^+/K^+ ATPase detection B. CFTR expression of the total

protein fraction from CFBE F508del cells, grown on plastic dish, after 24h-incubation with VX661 (18µM), VX445 (3µM) and VX770 (1µM) as indicated above blot (representative blot of 2 independent experiments). Equal protein loading was controlled via Na^+/K^+ ATPase detection C. Results of densitometric analysis of blots illustrated in A expressed as ratio of mature form C to the sum of forms B + C from CFBE F508del and CFBE WT cells (n=6). Results are presented as mean ± SEM. Statistics are versus DMSO control (*$P< 0.05$; ***$P<$ 0.001 and ****$P< 0.0001$) or versus 2VX treatment (#$P< 0.05$)

Figure 4

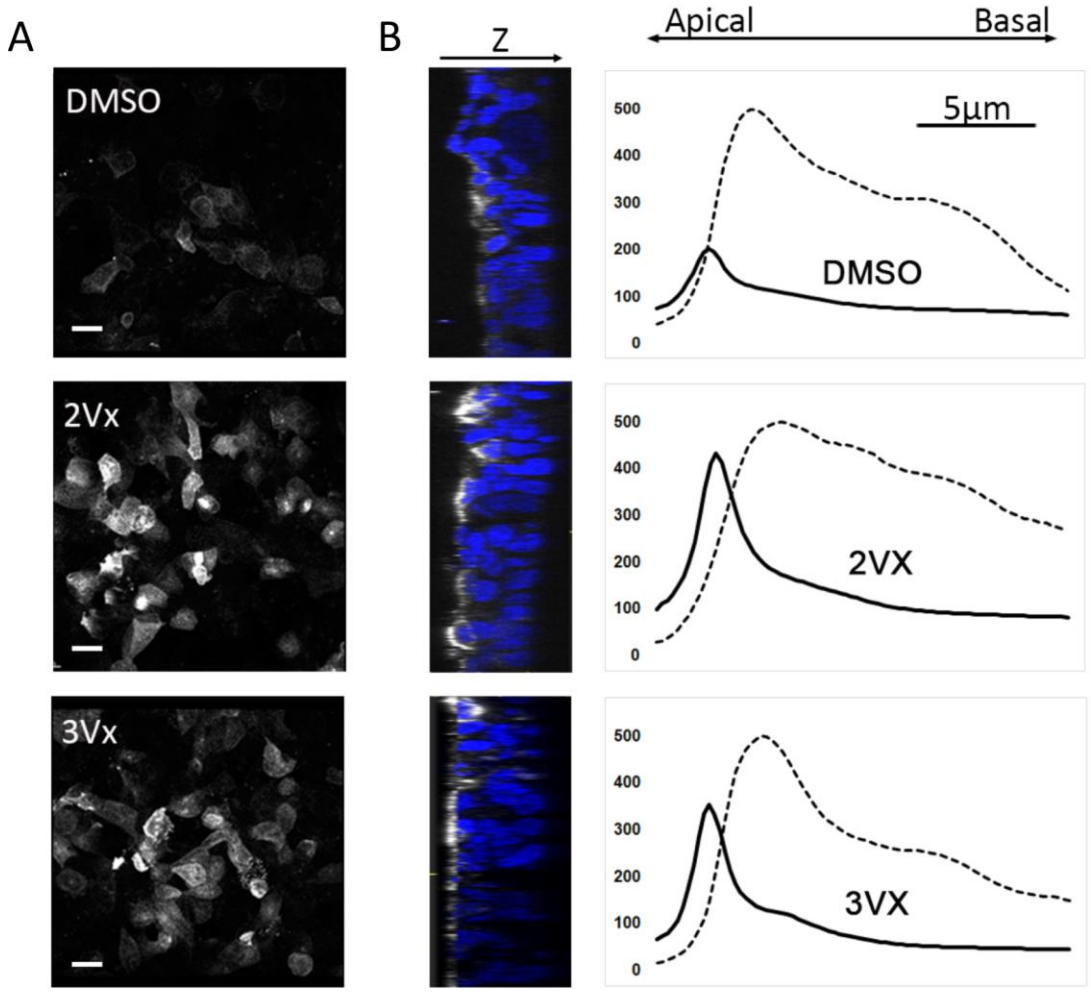
A
B
Z
Apical
Basal
DMSO
2Vx
3Vx
5µm
500
400
300
200
100
0
DMSO
2VX
3VX

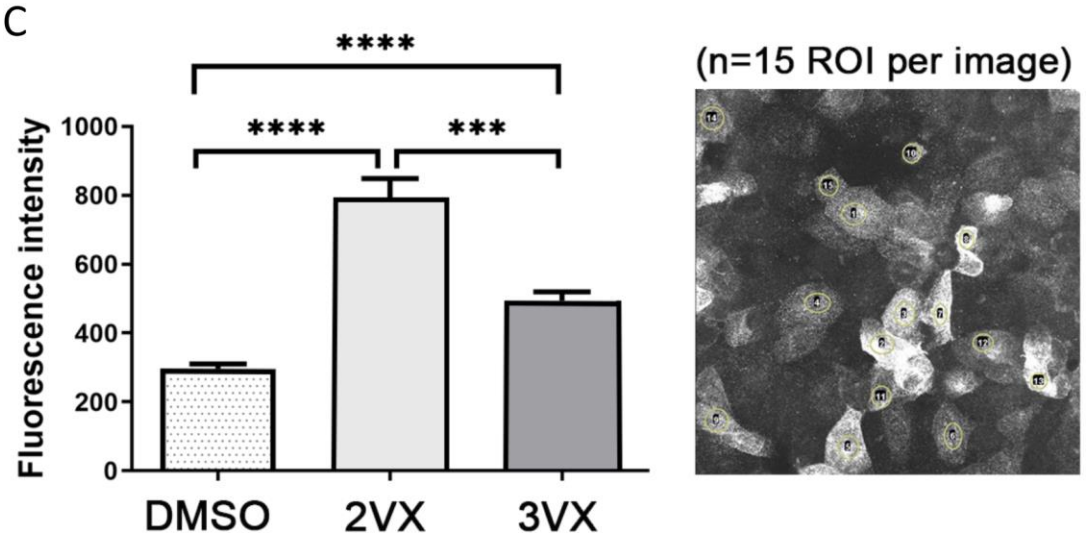
C
****
****
***
Fluorescence intensity
1000
800
600
400
200
0
DMSO
2VX
3VX
(n=15 ROI per image)

Figure 4. Effect of correctors on CFTR membrane localization on polarized cultured of CFBE F508del epithelial cells. A. Representative confocal images showing level of F508del-CFTR immuno-fluorescent staining after 24h-incubation with DMSO, 2VX or 3VX. Images are maximum intensity projection of Z-stack (scale bar 20 µm). B. Representative Z section of 3D confocal images showing apical localization of CFTR staining along thickness of 3D culture (2 to 3 cell layers were revealed with DAPI staining). On the right, graphs represent localization of CFTR (revealed with AF647 coupled antibody, solid lines) and nuclei (stained with DAPI, dotted lines) from apical to basal Z position. For each experimental condition, curves were obtained from fluorescence mean intensity values calculated along Z series (0.2 µm Z step, 5 images per condition, 15 ROI per image). C. Mean intensity of fluorescence measured from Z maximum intensity projection images. As shown at the right side of the graph, minimum 15 ROI were defined on enhanced contrast display image. Results are presented as mean ± SEM. Statistical analysis was performed by multiple comparisons using Mann Whitney tests (*** *P<0.001*, **** *P<0.0001*).

Figure 5

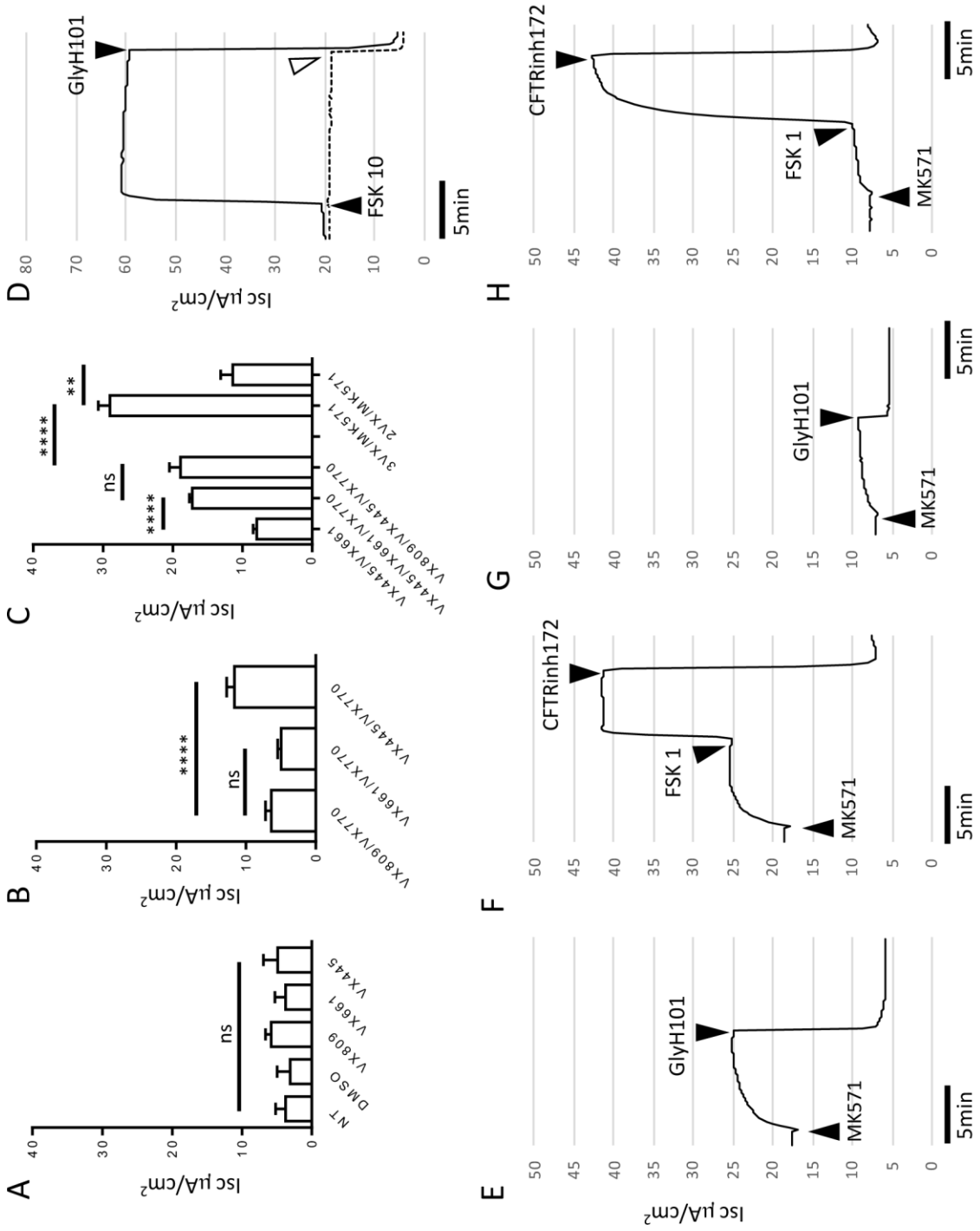
A
B
C
D
E
F
G
H
Isc µA/cm²
NT
DMSO
VX809
VX661
VX445
ns
VX809/VX770
VX661/VX770
VX445/VX770
****
VX445/VX661
VX445/VX661/VX770
VX809/VX445/VX770
3VX/MK571
2VX/MK571
**
GlyH101
FSK 10
5min
CFTRinh172
FSK 1
MK571

Figure 5. Determination of the basal Isc. A, C. Averaged basal Isc currents before FSK stimulation for each treatment condition on CFBE F508del cells. Results are presented as mean ± SEM. ns, no significant difference; ***P< 0.01* and ********P< 0.0001*. D. Two superposed original tracings showing Isc for CFBE F508del cells incubated with elexacaftor/tezacaftor/ivacaftor and stimulated by FSK (10 µM) (arrow, solid line) or not (dotted line). The CFTR inhibitor GlyH-101 (15 µM) was used to block Isc (second full and empty arrows). E-H. Original tracings showing Isc with CFBE F508del cells incubated with Trikafta (E, F) and elexacaftor/tezacaftor (G, H). Isc was stimulated by the MRP4 inhibitor MK571 (20 µM). FSK was used at 1µM in F and H. To block CFTR-dependent Isc we used either GlyH-101 (15 µM, E and G) or CFTRinh172 (10 µM, F and H). Arrows indicate when we added agents.

Figure 6

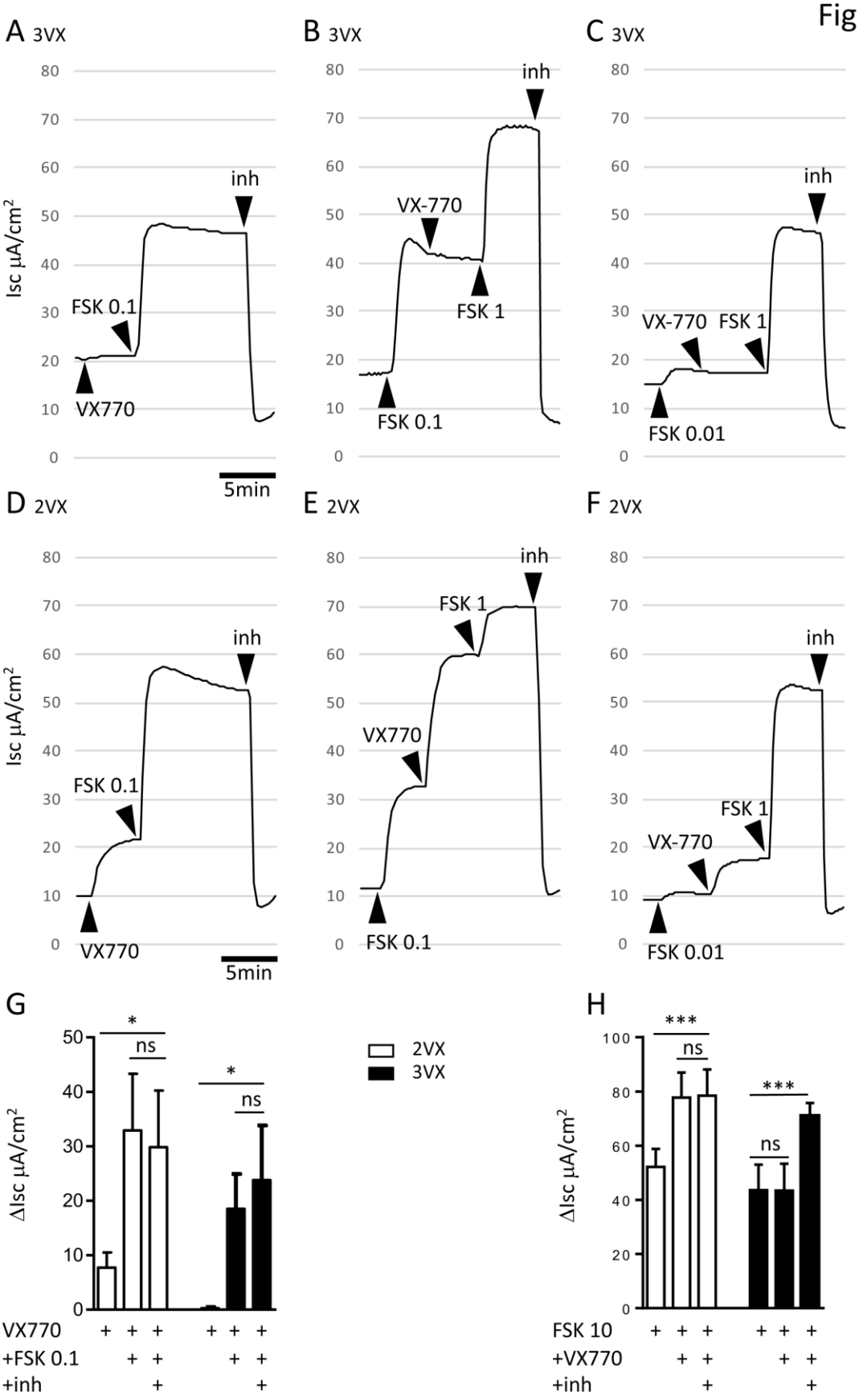
A 3VX
B 3VX
C 3VX
D 2VX
E 2VX
F 2VX
Isc µA/cm²
FSK 0.1
VX770
inh
5min
VX-770
FSK 1
FSK 0.01
G
H
2VX
3VX
ΔIsc µA/cm²
ns
*
***
VX770
+FSK 0.1
+inh
FSK 10
+VX770

Figure 6. Acute VX770 stimulates F508del-Isc in elexacaftor/tezacaftor but not in Trikafta treated cells. A-F. Original tracings showing Isc for CFBE F508del cells treated by elexacaftor/tezacaftor/ivacaftor (A-C) or elexacaftor/tezacaftor (D-F). The Isc current was stimulated by different combinations of VX770 (1 µM) and FSK (0.01, 0.1 or 1 µM as indicated). The concentrations are indicated on each plot. Inh: CFTRinh172 (10 µM). G, H. Mean ± SEM of ΔIsc as indicated under each bar histogram (n=4-8). ns, no significant difference; *$P< 0.05$ and ***$P< 0.001$.

Figure 7

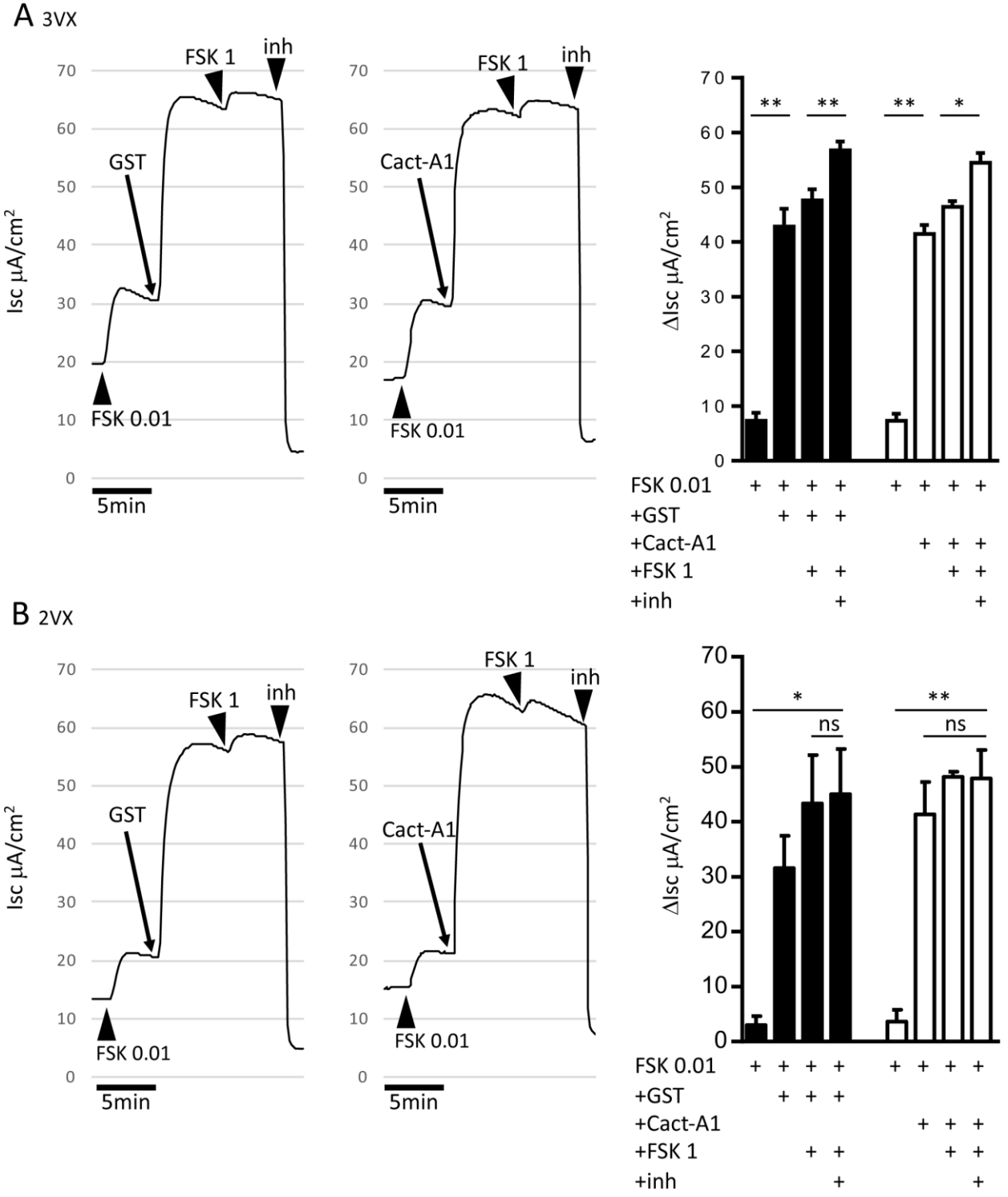
A 3VX
Isc µA/cm²
FSK 1
inh
GST
FSK 0.01
5min
Cact-A1
ΔIsc µA/cm²
FSK 0.01
+GST
+Cact-A1
+FSK 1
+inh
B 2VX
ns

Figure 7. Genistein and Cact-A1 stimulate F508del-Isc in elexacaftor/tezacaftor and in Trikafta treated cells. A, B. Original tracings showing Isc for CFBE F508del cells treated by elexacaftor/tezacaftor/ivacaftor (A) or elexacaftor/tezacaftor (B). Isc currents stimulated by different combinations of FSK, genistein (GST, 30 µM) and Cact-A1 (30 µM). Inh: CFTRinh172 (10 µM). In A (n=5) and B (n=4), the histograms on the right show the mean ± SEM of ΔIsc. ns, no significant difference; **P< 0.05* and ***P< 0.01*.

Figure 8

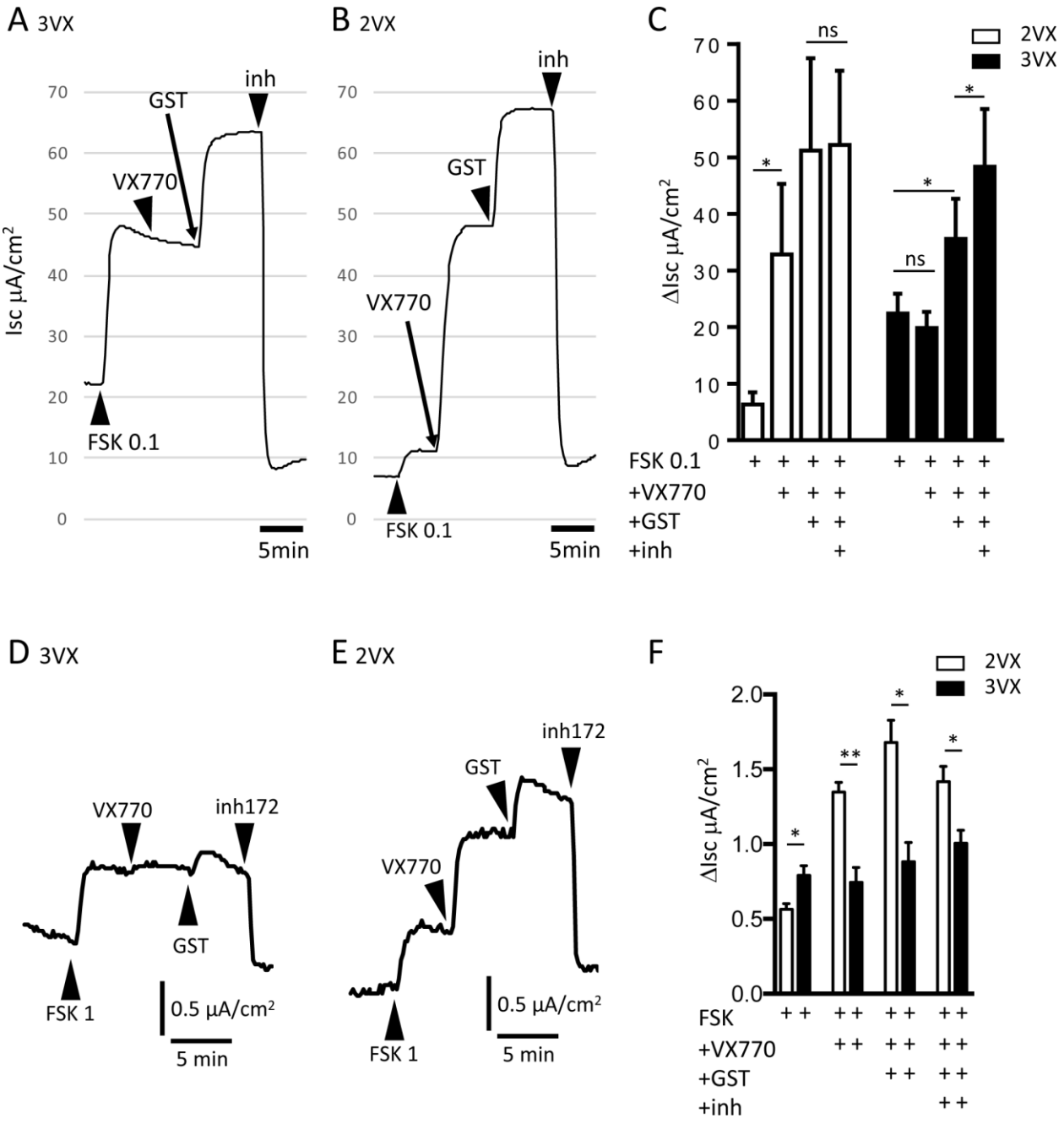
A 3VX
B 2VX
C
Isc µA/cm²
ΔIsc µA/cm²
GST
inh
VX770
FSK 0.1
5min
ns
2VX
3VX
+VX770
+GST
+inh
D 3VX
E 2VX
F
inh172
FSK 1
0.5 µA/cm²
5 min
FSK

Figure 8. Genistein added after VX770 stimulates F508del-Isc in elexacaftor/tezacaftor and Trikafta treated cells. A, B. Original tracings showing Isc for CFBE F508del cells treated by elexacaftor/tezacaftor/ivacaftor (A) and elexacaftor/tezacaftor (B). C. Mean ± SEM of ΔIsc (n=4-5) in response to FSK (0.1 µM), VX770 (1 µM) and genistein (GST, 30 µM). Inh: CFTRinh172 (10 µM) as indicated below each bar histogram. D, E. Original tracings showing Isc for HAE F508del cells treated by elexacaftor/tezacaftor/ivacaftor (D) and elexacaftor/tezacaftor (E). F. Mean ± SEM of ΔIsc (n=3) in response to FSK (1 µM), VX770 (1 µM) and genistein (GST, 30 µM) as indicated below each bar histogram. Inh: CFTRinh172 (10 µM). ns, no significant difference; *$P< 0.05$ and **$P< 0.01$.

A

Lumacaftor (VX809)

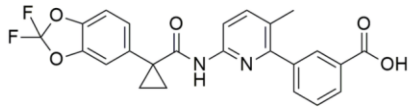

Tezacaftor (VX661)

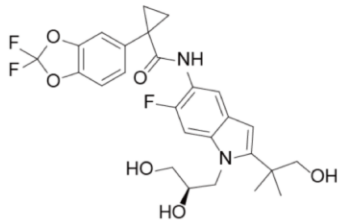

Elexacaftor (VX445)

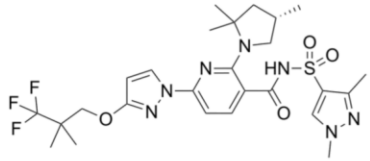

Ivacaftor (VX770)

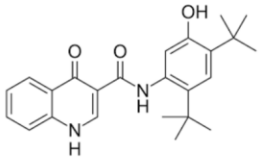

B

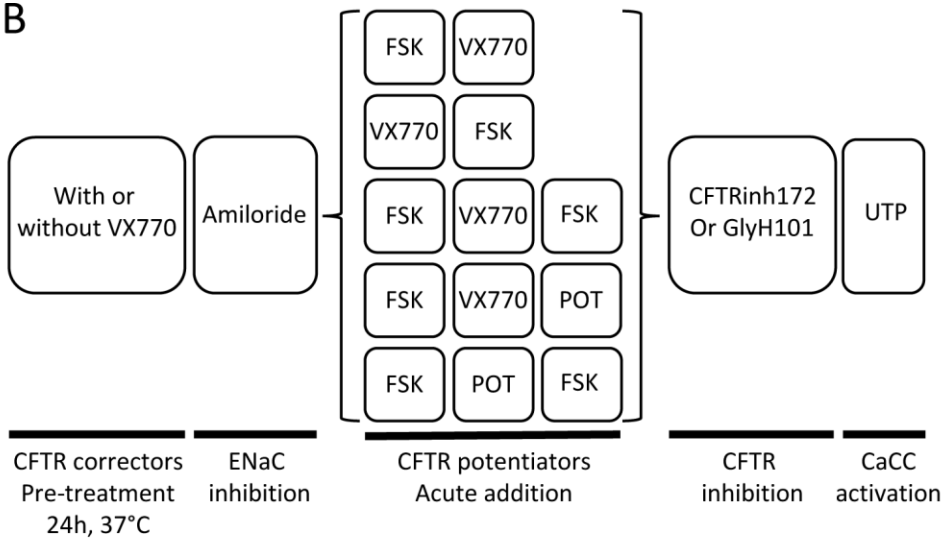

C

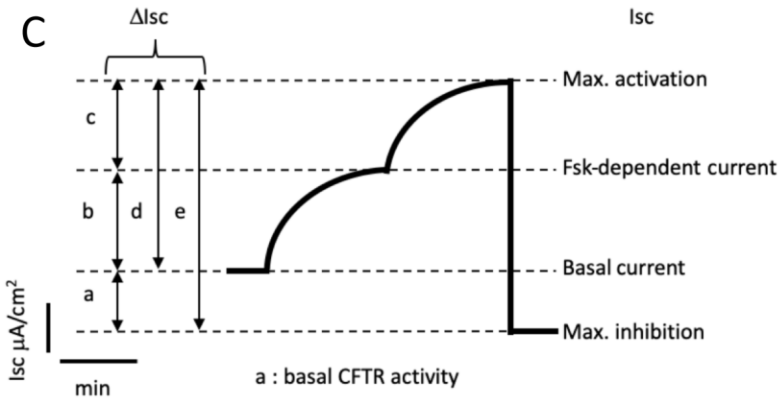

a : basal CFTR activity

b : forskolin-dependent CFTR ΔIsc

c : potentiator-dependent CFTR ΔIsc

d : activatable CFTR ΔIsc

e : inhibitable CFTR ΔIsc

Figure S1

Supplemental Figure S1. Chemicals and protocols A. chemical structures of the therapeutic correctors lumacaftor, tezacaftor and elexacaftor and of the potentiator ivacaftor. B. scheme illustrating the protocols used to record Isc in airway epithelial cells. POT: genistein or Cact-A1. C. scheme showing the analysis of Isc to determine basal Isc (a), forskolin (b) and potentiator (c)-dependent ΔIsc, activatable (d) and inhibitable (e) CFTR ΔIsc.

Figure S2

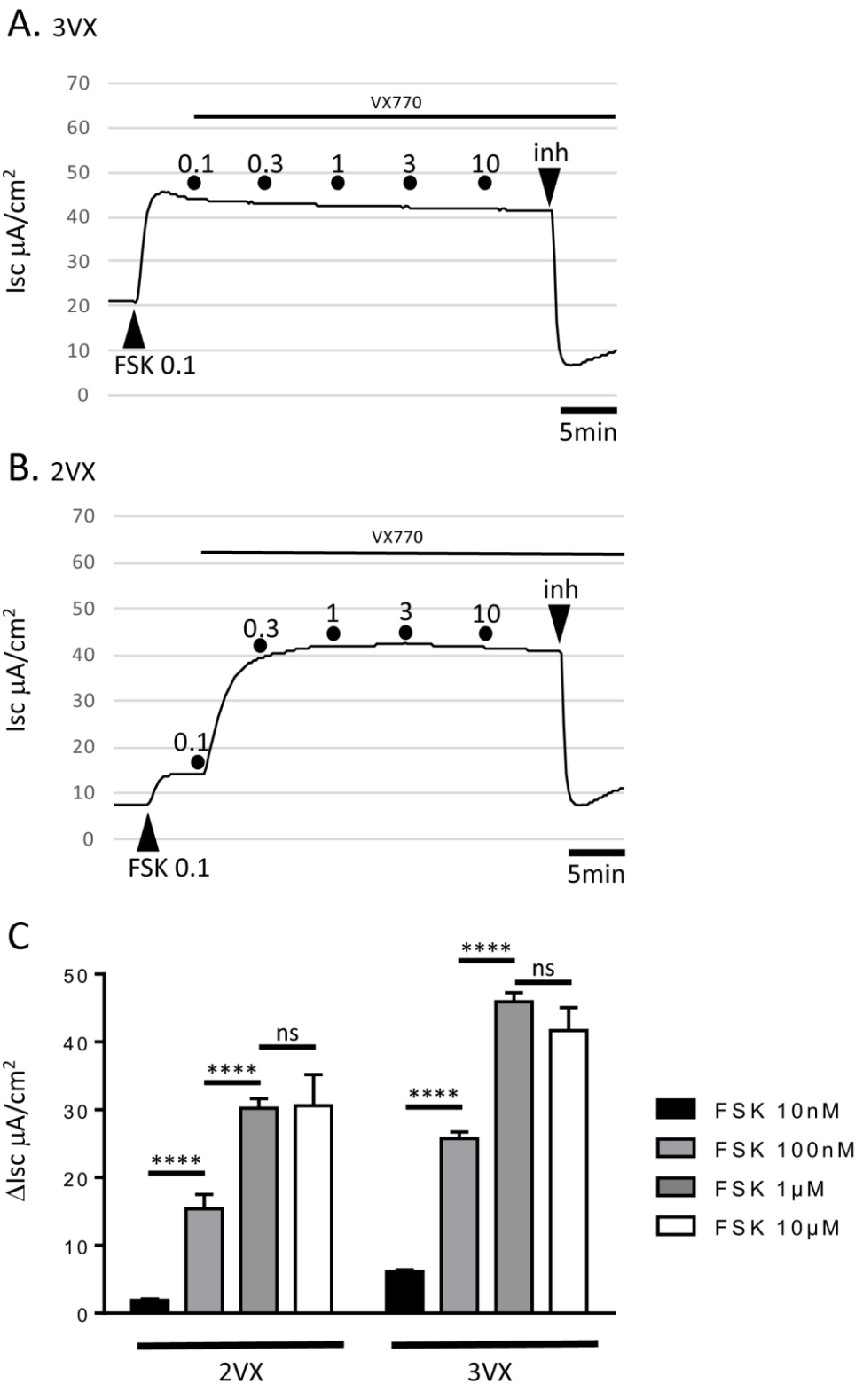
A. 3VX
Isc µA/cm²
70
60
50
40
30
20
10
0
VX770
0.1
0.3
1
3
10
inh
FSK 0.1
5min
B. 2VX
Isc µA/cm²
VX770
inh
0.3
1
3
10
0.1
FSK 0.1
5min
C
ΔIsc µA/cm²
50
40
30
20
10
0
****
****
ns
****
****
ns
2VX
3VX
FSK 10nM
FSK 100nM
FSK 1µM
FSK 10µM

Supplemental Figure S2. Stimulation of F508del-Isc by VX770 and forskolin. A, B. Original tracings showing Isc with CFBE F508del cells incubated by elexacaftor/tezacaftor/ivacaftor (noted 3VX in A) or elexacaftor/tezacaftor (noted 2VX in B). The Isc CFTR current was stimulated by FSK (0.1 µM, arrow) then VX770 (increasing concentrations as indicated by the dot on the traces) then inhibited by 10 µM CFTRinh172 (inh, second arrow). C. Mean ± SEM of ΔIsc in response to increasing concentrations of FSK (n=4-8 for each concentration). ns, no significant difference and ****$P< 0.0001$.

Figure S3

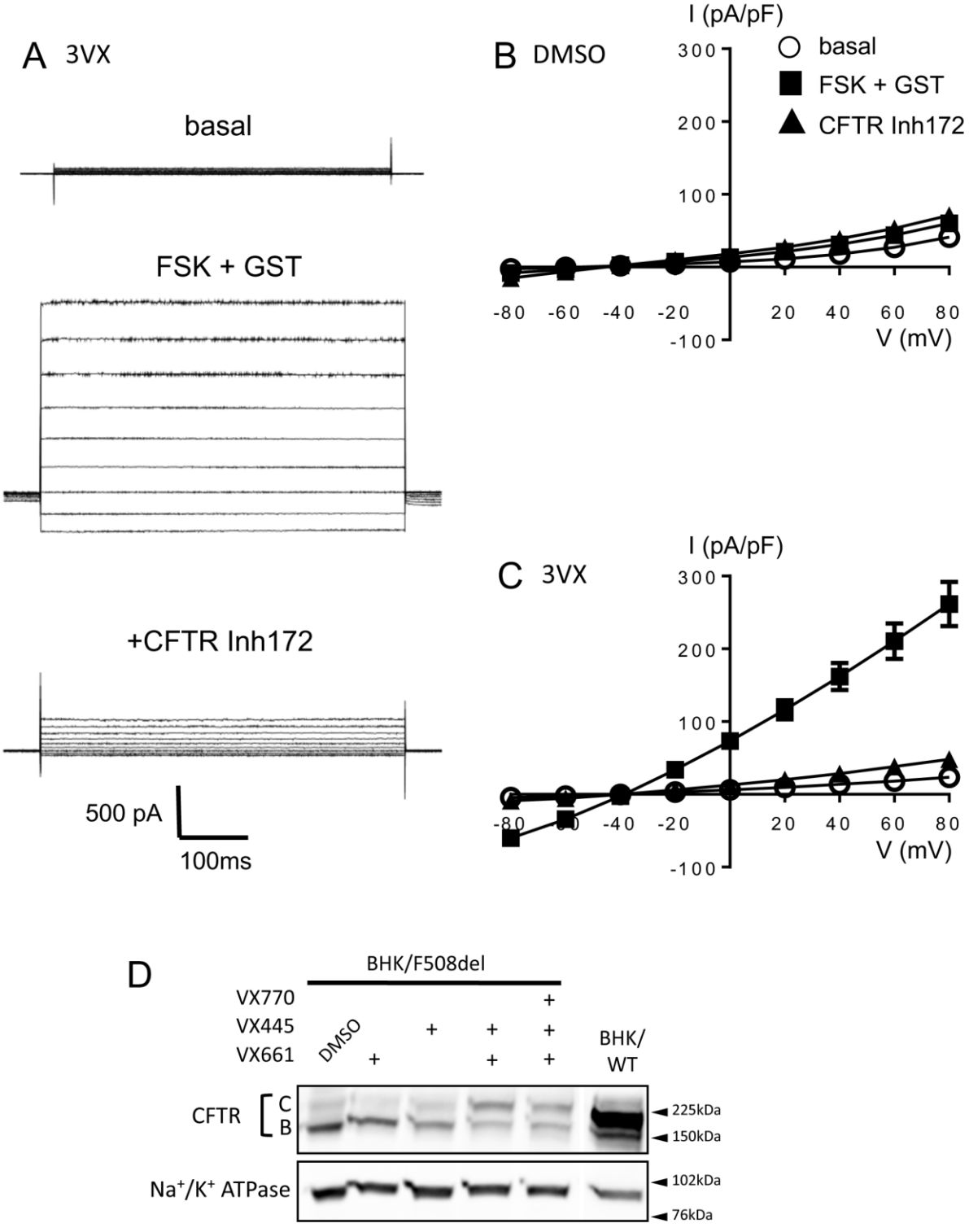
A 3VX
basal
FSK + GST
+CFTR Inh172
500 pA
100ms
B DMSO
I (pA/pF)
basal
FSK + GST
CFTR Inh172
300
200
100
-100
-80 -60 -40 -20 20 40 60 80
V (mV)
C 3VX
I (pA/pF)
300
200
100
-100
-40 -20 20 40 60 80
V (mV)
D
BHK/F508del
VX770
VX445
VX661
DMSO
BHK/
WT
CFTR
C
B
225kDa
150kDa
Na+/K+ ATPase
102kDa
76kDa

Supplemental Figure S3. Whole-cell patch clamp recordings of F508del chloride currents in BHK cells A. Original tracings of whole-cell F508del-CFTR chloride currents in basal (upper traces), after adding FSK (10 µM) + GST (30 µM) (middle traces) and after adding CFTRinh172 (10 µM) (bottom traces). B, C. Current density/V relationships for non-treated BHK cells (n=14, B) or BHK cells treated by elexacaftor/tezacaftor/ivacaftor (n=15, C). Basal is indicated by circles, FSK+GST by squares and CFTRinh172 by triangles. D. CFTR expression of the total protein fraction from BHK F508del cells after 24h-incubation with VX661 (18 µM), VX445 (3 µM) and VX770 (1 µM) alone or in combination or DMSO control as indicated above blot and of BHK WT cells grown on dish (representative blot of 2 independent experiments). Equal protein loading was controlled via Na^+/K^+ ATPase detection.

CFTR Modulators	Market Name USA EU	Year Approved USA (FDA*) EU (EMA*)	Indication (age)	CF mutations	CF Population	Lung ppFEV1**	Lung exacerbation reduction	Estimated annual cost US ($) EU (€)
Ivacaftor	Kalydeko	2012 2014	>6 mo	Class III, gating mutation, residual function and conduction mutations (class IV)	3-5%	10.6-12.5% (week 24)	55%	311000 260000
Lumacaftor /Ivacaftor	Orkambi	2015 2018	>12 yr >6 yr	Class II, F508del homozygous	45-50%	2.6-4.0%	30-39%	272000 226000
Tezacaftor/Ivacaftor with Ivacaftor	Symdeko Symkevi	2018 2018	>6 yr	Class II, F508del homozygous, heterozygous, other mutations	45-50%	4.0-6.8%	35%	292000 242000
Elexacaftor/ Tezacaftor/ Ivacaftor with Ivacaftor	Trikafta Kaftrio	2019 2020	>6 yr	Class II, at least one copy of F508del mutation and one copy with residual function mutation	85-90%	10.4-13.8%	63%	311000 260000

* FDA: Food and Drug Administration; EMA: European Medicines Agency;

**ppFEV1: percent predicted forced expiratory volume in 1 second

Table 1. Therapeutic CFTR modulators